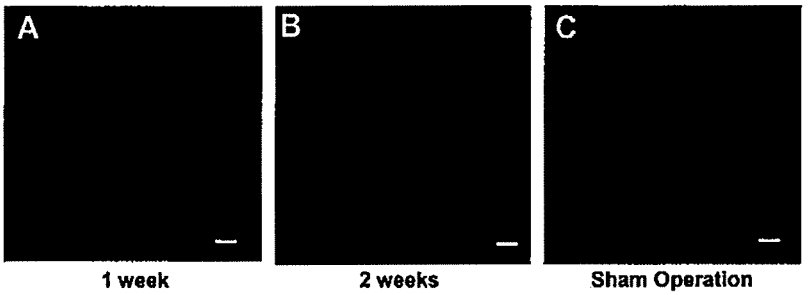

Fig. 1. BM-derived GFP-positive cells in the vascular remodeling lesion of LDL−/− mouse. A–C, Representative microscopic photographs of BM-derived GFP-positive cells in the vascular remodeling lesion of LDL−/− mouse. Four weeks after BMT, a non-constrictive polyethylene cuff was placed around the right femoral artery in four mice in each group. The cuffed (A, 1 week after cuff placement; B, 2 weeks after cuff placement) or sham-operated (C) femoral arteries were examined under fluorescence microscopy. Scale bars: 100 μm.

levels, the fractions of the cross-sectional area covered by remodeling lesions were significantly larger in mice fed a high-fat diet than those fed a normal chow diet ($23.0 \pm 8.68\%$ vs. $2.11 \pm 1.17\%$, $P < 0.01$, $n = 4$ in each group). These results indicate that hypercholesterolemia can increase intimal lesion formation in cuff-induced vascular injury.

Hypercholesterolemia induced foam cell formation in the intima and media in a cuff model

In this model, we found that atherosclerosis-like lesions, predominantly consisting of a massive accumulation of foam cells in the intima and media at 2 weeks after cuff placement (Fig. 2B), but no neointima formation was found at 1 week after cuff placement (Fig. 2A). At 1 week after cuff placement, we could hardly detect any neointima formation, where we just observed some foam cells in the adventitia. We also found that the media was hyperplastic and clearly stained with Oil red O, indicating a plenty of cholesterol accumulation in the media while the intimal thickening was formed 2 weeks after cuff placement. To identify the cell lineage in the lesions, we stained the tissue with anti-MOMA-2 and anti-1A4 antibodies. We found that MOMA-2 and Oil red O-positive cells were accumulated at neointima and media (Fig. 2C) and that 1A4-positive SMCs were localized on top of macrophages (Fig. 2D), as a sign of cap formation. The deposition of foam cells and SMCs occurred between the endothelial layer and the internal elastic lamina.

Macrophages play an important role in the intimal and medial thickening after cuff placement

In the presence of hypercholesterolemia, numerous macrophages were accumulated in the lesion area when the artery was injured by cuff placement. When the tissue stained with MOMA-2, we found many cells recruited to the adventitia and neointima. As expected, MOMA-2-positive cells were GFP-positive in the cuff-induced vascular remodeling lesion (data not shown).

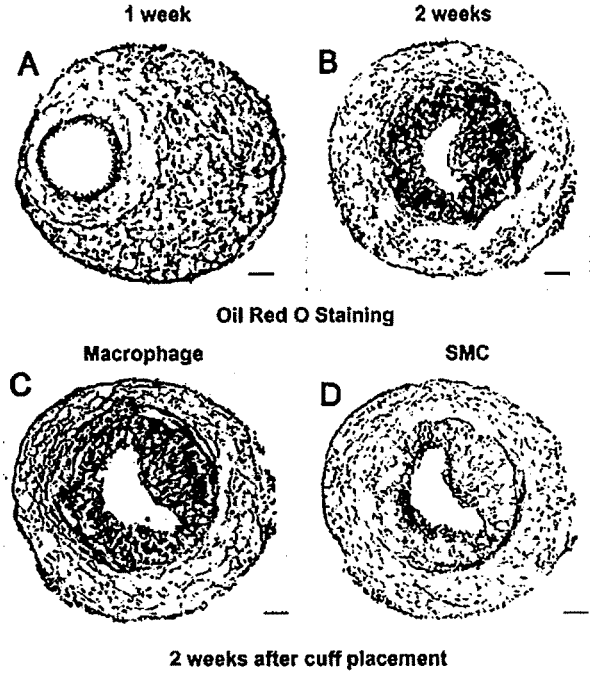

Fig. 2. Effect of hypercholesterolemia on foam cells accumulation and the recruitment of macrophages and SMCs in cuff-induced vascular remodeling lesion. After the same procedure in Fig. 1, tissues were stained with Oil red O and hematoxylin. A large number of foam cells were observed in the lesion area at 1 week (A, adventitia) and 2 weeks (B, adventitia and neointima) after cuff placement. Tissues were also subjected to immunohistochemistry with antibodies to MOMA-2 (C) or αSMA (D). Scale bars: 100 μm.

BM cells can differentiate into vascular SMCs

To examine whether BM-derived cells can differentiate into SMCs in the vascular remodeling lesion, we stained the tissue with Cy3-labeled anti-αSMA (clone 1A4) antibody. We found a number of 1A4-positive cells in the intimal lesion area (Fig. 3H and K) and that many 1A4-positive cells were also positive for GFP (Fig. 3I and L), indicating that BM-derived cells can differentiate into SMCs in the cuff-induced vascular remodeling lesion. However, in the earlier time point at 1 week after cuff

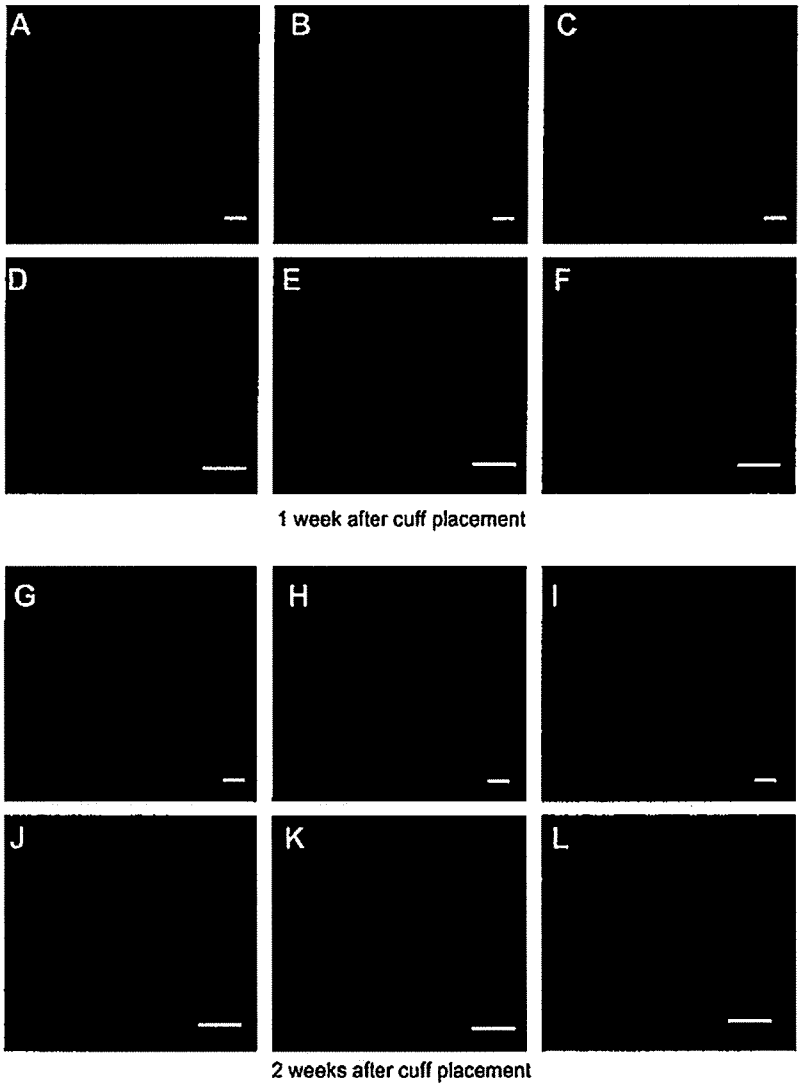

Fig. 3. BM-derived SMCs in LDL−/− mouse vascular remodeling lesion. After the same procedure in Fig. 1, tissues were subjected to immunohistochemistry with Cy3-labeled antibody for αSMA (B, E, H, and K). (A, D, G, and J) Fluorescent microscopic photographs for GFP. (A–F) Fluorescent microscopic photographs from femoral artery of 1 week after cuff placement. All the others are samples at 2 weeks after cuff placement. (C, F, I, and L) Merged images of GFP and Cy3 signals from (A) and (B), (D) and (E), (G) and (H), and (J) and (K), respectively. Scale bars: 100 μm.

placement, we could find few SMCs in vascular remodeling lesion (Fig. 3C and F).

Endothelial progenitor cells (EPCs) are recruited to the cuffed vascular remodeling lesion

Because it is unknown whether hypercholesterolemia can increase EPC recruitment to the cuff-induced vascular remodeling lesion, we performed endothelial staining by anti-CD31 antibody. We found that the endothelial lining of the intima was clearly stained with anti-CD31 antibody, and that plenty of small vessels in the adventitia were also stained (Fig. 4C ,F , I, and L). Many clustered cells in small vessels in the adventitia were positive for CD31 and GFP, indicating the involvement of angiogenesis from BM-derived cells. However, at 1 week after cuff placement, more EPCs could be found in the vascular remodeling lesion at this earlier phase than SMCs (Fig. 4C and F).

Discussion

In this study, we have shown that hypercholesterolemia could induce intimal lesion formation after placement of a non-constrictive polyethylene cuff around the femoral artery in LDL−/− mice. Although previous investigators have shown intimal thickening in the cuff-induced vascular injury model [10–12], we have not been able to reproduce their results in our previous experiment in normal C57BL/6 mice [6]. However, in this study, we successfully induced intimal hyperplasia and vascular remodeling in

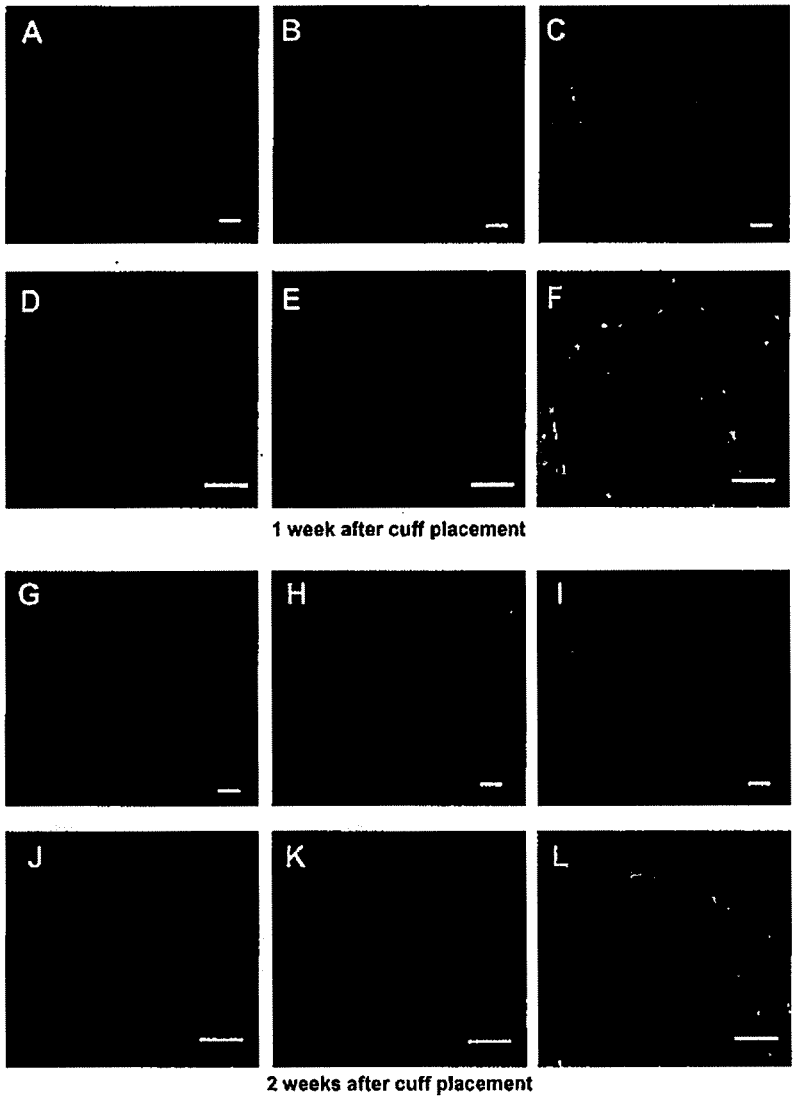

Fig. 4. BM-derived EPCs in cuff-induced vascular remodeling lesions. After the same procedure in Fig. 1, tissues were subjected to immunostaining with anti-CD31 antibody. (A–F) From the tissue at 1 week after cuff placement, and (G–L) From the tissue at 2 weeks after cuff placement. (A, D, G, and J) GFP signals, (B, E, H, and K) CD31 signals, and (C, F, I, and L) merged images of GFP and CD31 signal from (A) and (B), (D) and (E), (G) and (H), and (J) and (K), respectively. Scale bars: 100 μm.

an atherogenic model in a short period of time. A previous study has reported that hyperlipidemia causes progressive atherosclerosis [3,13]. In our study, the atherosclerotic-like lesion was occurred in cuff-planted femoral artery in LDL−/− mice in the present of hypercholesterolemia. This result indicates that hypercholesterolemia is a major factor in the intimal lesion formation after vascular injury.

We observed numerous foamy macrophages in the adventitia in 1 week in this model. However, in this period, intimal lesion formation did not develop even though the plasma cholesterol was high enough. After 2 weeks of cuff placement, there were numerous foam cells accumulated in the media as well as in the intima. In addition, because atherosclerotic lesions, which develop spontaneously in transgenic mice, are frequently located in the central part of the arterial tree, local anti-atherosclerotic strategies are difficult to apply. Therefore, the induction of atherosclerotic-like lesions within several weeks, at a predefined, easily accessible site in the arterial tree, with a known onset in time, would be preferable for studying factors causing the early onset of atherosclerotic lesions and for assessing the effect of systemic and local anti-atherosclerotic therapies. As shown in this study, the cuff model for accelerated atherosclerotic lesions is suitable for studying the early steps in atherosclerotic plaque formation. Moreover, accelerated atherosclerosis observed in human vein grafts, with less organized structures lacking typical features such as the fibrous cap and necrotic core, shows high morphological resemblance to the atherosclerotic lesions observed in this model [14].

In the previous study, we observed that numerous BM-derived macrophages and SMCs were recruited to the adventitia after vascular injury in C57BL/6 mice [6]. Similar to the previous study, it is clearly shown that BM-derived macrophages, SMCs, and ECs contributed to the lesion formation after cuff placement. We found that almost all of SMCs in the intima and the most part of ECs in the perivascular remodeling lesion were derived from BM. This result indicates that hypercholesterolemia not only could accelerate the intimal lesion formation, but also affect the recruitment of BM-derived cells after vascular injury. Although we did not compare the number of cells positive for CD31 and GFP quantitatively, the number of these cells seemed to increase compared with that without high-fat diet in our previous study.

Schmeisser et al. reported that BM-derived macrophages might contribute to neovascularization by in situ transdifferentiation to EC-like cells [15]. We found that in the vascular injury lesion there were many cells positive for endothelial marker CD31 at 1 week and 2 weeks after cuff placement. Furthermore, most of the cells forming a small vessel were positive for CD31 and GFP, indicating that the source of the ECs forming a small vessel in the adventitia is from BM.

Limitation of this study is a lack of the mechanistic insights. We could not provide evidence to explain the mechanism of vascular remodeling modified by hypercholesterolemia. Further study is necessary to address this point.

In summary, we have successfully developed the atherosclerotic-like lesions after cuff-induced vascular injury in LDL−/− mice in the presence of hypercholesterolemia. Hypercholesterolemia may have an important role in recruitment of BM-derived cells to vascular remodeling lesions.

Acknowledgments

This study was supported by Grants-in-Aid from the Ministry of Education, Culture, Science, Sports, and Technology of Japan. We have no duality of interest to declare.

References

[1] J.H. Ip, V. Fuster, L. Badimon, J. Badimon, M.B. Taubman, J.H. Chesebro, Syndromes of accelerated atherosclerosis: role of vascular injury and smooth muscle cell proliferation, J. Am. Coll. Cardiol. 15 (1990) 1667–1687.

[2] M.G. Davies, P.O. Hagen, Pathophysiology of vein graft failure: a review, Eur. J. Vasc. Endovasc. Surg. 9 (1995) 7–18.

[3] R. Ross, L. Harker, Hyperlipidemia and atherosclerosis, Science 193 (1976) 1094–1100.

[4] R. Ross, Atherosclerosis—an inflammatory disease, N. Engl. J. Med. 340 (1999) 115–126.

[5] P. Libby, Inflammation in atherosclerosis, Nature 420 (2002) 868–874.

[6] Y. Xu, H. Arai, X. Zhuge, H. Sano, T. Murayama, M. Yoshimoto, T. Heike, T. Nakahata, S. Nishikawa, T. Kita, M. Yokode, Role of bone marrow-derived progenitor cells in cuff-induced vascular injury in mice, Arterioscler. Thromb. Vasc. Biol. 24 (2004) 477–482.

[7] T. Murayama, M. Yokode, H. Kataoka, T. Imabayashi, H. Yoshida, H. Sano, S. Nishikawa, T. Kita, Intraperitoneal administration of anti-c-fms monoclonal antibody prevents initial events of atherogenesis but does not reduce the size of advanced lesions in apolipoprotein E-deficient mice, Circulation 99 (1999) 1740–1746.

[8] A. Nicoletti, S. Kaveri, G. Caligiuri, J. Bariety, G.K. Hansson, Immunoglobulin treatment reduces atherosclerosis in apo E knockout mice, J. Clin. Invest. 102 (1998) 910–918.

[9] H. Sano, T. Sudo, M. Yokode, T. Murayama, H. Kataoka, N. Takakura, S. Nishikawa, S.I. Nishikawa, T. Kita, Functional blockade of platelet-derived growth factor receptor-beta but not of receptor-alpha prevents vascular smooth muscle cell accumulation in fibrous cap lesions in apolipoprotein E-deficient mice, Circulation 103 (2001) 2955–2960.

[10] M. Moroi, L. Zhang, T. Yasuda, R. Virmani, H.K. Gold, M.C. Fishman, P.L. Huang, Interaction of genetic deficiency of endothelial nitric oxide, gender, and pregnancy in vascular response to injury in mice, J. Clin. Invest. 101 (1998) 1225–1232.

[11] H.W. Liu, M. Iwai, Y. Takeda-Matsubara, L. Wu, J.M. Li, M. Okumura, T.X. Cui, M. Horiuchi, Effect of estrogen and AT1 receptor blocker on neointima formation, Hypertension 40 (2002) 451–457 (discussion 448–450).

[12] J. Suzuki, M. Iwai, H. Nakagami, L. Wu, R. Chen, T. Sugaya, M. Hamada, K. Hiwada, M. Horiuchi, Role of angiotensin II-regulated apoptosis through distinct AT1 and AT2 receptors in neointimal formation, Circulation 106 (2002) 847–853.

[13] C.R. Minick, M.B. Stemerman, W. Insull Jr., Role of endothelium and hypercholesterolemia in intimal thickening and lipid accumulation, Am. J. Pathol. 95 (1979) 131–158.

[14] J.G. Motwani, E.J. Topol, Aortocoronary saphenous vein graft disease: pathogenesis, predisposition, and prevention, Circulation 97 (1998) 916–931.

[15] A. Schmeisser, C.D. Garlichs, H. Zhang, S. Eskafi, C. Graffy, J. Ludwig, R.H. Strasser, W.G. Daniel, Monocytes coexpress endothelial and macrophagocytic lineage markers and form cord-like structures in Matrigel under angiogenic conditions, Cardiovasc. Res. 49 (2001) 671–680.

Critical Role for CXC Chemokine Ligand 16 (SR-PSOX) in Th1 Response Mediated by NKT Cells[1]

Takeshi Shimaoka,*† Ken-ichiro Seino,‡§ Noriaki Kume,¶ Manabu Minami,¶ Chiyoko Nishime,‖ Makoto Suematsu,‖ Toru Kita,¶ Masaru Taniguchi,‡ Kouji Matsushima,† and Shin Yonehara[2]*

The transmembrane chemokine CXCL 16 (CXCL16), which is the same molecule as the scavenger receptor that binds phosphatidylserine and oxidized lipoprotein (SR-PSOX), has been shown to mediate chemotaxis and adhesion of CXC chemokine receptor 6-expressing cells such as NKT and activated Th1 cells. We generated SR-PSOX/CXCL16-deficient mice and examined the role of this chemokine in vivo. The mutant mice showed a reduced number of liver NKT cells, and decreased production of IFN-γ and IL-4 by administration of α-galactosylceramide (αGalCer). Of note, the αGalCer-induced production of IFN-γ was more severely impaired than the production of IL-4 in SR-PSOX-deficient mice. In this context, SR-PSOX-deficient mice showed impaired sensitivity to αGalCer-induced anti-tumor effect mediated by IFN-γ from NKT cells. NKT cells from wild-type mice showed impaired production of IFN-γ, but not IL-4, after their culture with αGalCer and APCs from mutant mice. Moreover, *Propionibacterium acnes*-induced in vivo Th1 responses were severely impaired in SR-PSOX-deficient as well as NKT KO mice. Taken together, SR-PSOX/CXCL16 plays an important role in not only the production of IFN-γ by NKT cells, but also promotion of Th1-inclined immune responses mediated by NKT cells. *The Journal of Immunology*, 2007, 179: 8172–8179.

NKT cells, which coexpress NK1.1 and TCR on their surface, differ from conventional T and NK cells expressing TCR and NK1.1, respectively. NKT cells, most of which express an invariant TCR containing Vα14-Jα281, were shown to specifically recognize glycolipids such as α-galactosylceramide (αGalCer)[3] and isoglobotrihexosylceramide (iGb3) presented by CD1d on APCs. NKT cells are generated in the thymus and distributed to the thymus, spleen, liver and bone marrow. NKT cells are highly concentrated in the liver where they account for ~20% of lymphocytes, compared with <1% in other organs (1–3). A hallmark of NKT cells is the rapid production of large amounts of IFN-γ and/or IL-4 after stimulation with αGalCer, regulating the development of Th1 and Th2 cells, respectively (2).

NKT cells were reported to play an important role in host defense against infection with bacteria, virus and protozoan parasite (4) and NKT cell-induced IFN-γ was shown to be important in host defense to several types of infection (4). αGalCer-stimulated NKT cells was also shown to exert an anti-tumor effect by inducing IFN-γ (5, 6). These activities of NKT cells are mainly explained by the Th1 response induced by IFN-γ production by NKT cells. On the contrary, α-GalCer treatment was reported to protect NOD mice from autoimmune type I diabetes through stimulating a polarized Th2-like response; suppressing IFN-γ production and/or inducing IL-4 production by NKT cells (7–9). OCH, which is a truncated version of the prototypic NKT cell ligand α-GalCer, was reported to induce a predominant production of IL-4 by NKT cells, and to suppress experimental autoimmune encephalitis (EAE) through inducing Th2 bias of autoimmune T cells (10). Thus, NKT cells can control the development of Th1- and Th2-polarized immune responses by inducing Th1 and Th2 responses through the production of large amounts of IFN-γ and IL-4, respectively (2). It would be important to investigate the molecular and cellular mechanism by which NKT cells differentially produce cytokines (IFN-γ or IL-4). Recently, interaction of CD40 and CD154 on APCs and NKT cells, respectively, was reported to mediate production of IFN-γ but not of IL-4 by αGalCer-stimulated NKT cells, while interaction between CD28 and CD80/CD86 on NKT cells and APCs, respectively, was shown to be important for the production of both IFN-γ and IL-4 (11). LFA-1 was reported to function as a costimulatory molecule for αGalCer-activated NKT cells to produce IL-4 but not IFN-γ (12). However, the molecular mechanism has not been fully understood how NKT cells are regulated to specifically produce IFN-γ or IL-4 leading to generation of Th1 or Th2 cells, respectively.

The chemokine superfamily consists of small proteins that trigger directed migration of various types of leukocytes by specifically interacting with a group of seven transmembrane G protein-coupled receptors. In addition to this migration-inducing activity, chemokines also mediate signals that cause the activation of integrins and differentiation of target cells (13, 14). Recently, CXCL 16 (CXCL16)/SR-PSOX (scavenger receptor that binds phosphatidylserine and oxidized lipoprotein) has been characterized as a membrane-anchored chemokine specific for the G-protein coupled

*Graduate School of Biostudies, Kyoto University, Sakyo-ku, Kyoto, Japan; †Molecular Preventive Medicine, Graduate School of Medicine, University of Tokyo, Bunkyo-ku, Tokyo, Japan; ‡Research Center for Allergy and Immunology, The Institute of Physical and Chemical Research, Tsurumi-ku, Yokohama, Kanagawa, Japan; §Institute of Medical Science, St. Marianna University School of Medicine, Miyamae-ku, Kawasaki, Kanagawa, Japan; ¶Department of Cardiovascular Medicine, Graduate School of Medicine, Kyoto University, Sakyo-ku, Kyoto, Japan; and ‖School of Medicine, Keio University, Shinjuku-ku, Tokyo, Japan

Received for publication March 22, 2007. Accepted for publication October 1, 2007.

The costs of publication of this article were defrayed in part by the payment of page charges. This article must therefore be hereby marked *advertisement* in accordance with 18 U.S.C. Section 1734 solely to indicate this fact.

[1] This work was supported in part by Grants-in-Aid from the Ministry of Education, Culture, Sports, Science and Technology of Japan and from Solution Oriented Research for Science and Technology of Japan Science and Technology Corporation.

[2] Address correspondence and reprint requests to Dr. Shin Yonehara, Graduate School of Biostudies, Kyoto University, South Campus Research Building (Building G), Yoshida Konoe-cho, Sakyo-ku, Kyoto 606-8501, Japan. E-mail address: yonehara@lif.kyoto-u.ac.jp

[3] Abbreviations used in this paper: αGalCer, α-galactosylceramide; GPT, glutamic pyruvic transaminase; SR-PSOX, scavenger receptor that binds phosphatidylserine and oxidized lipoprotein.

 0022-1767/07/$2.00

receptor Bonzo/CXC chemokine receptor 6 (CXCR6) (15, 16) as well as a novel scavenger receptor for oxidized low density lipoprotein and bacteria (17, 18). SR-PSOX/CXCL16 is selectively expressed on APCs such as DCs and macrophages, and its receptor CXCR6 is expressed on NKT and activated Th1 cells (15, 16, 18–20). Furthermore, CXCR6-expressing effector T cells were shown to accumulate in type 1 inflammatory lesions such as rheumatoid joints and inflamed livers (20). In experimental autoimmune encephalitis (EAE), we showed that SR-PSOX/CXCL16 plays an important role in the elevation of the serum IFN-γ level during the primary immune response as well as recruitment of inflammatory mononuclear cells into the CNS, and administration of anti-SR-PSOX mAb decreased disease activity in both acute and transfer EAE (21). In a model of graft-vs-host disease, CXCR6-deficient activated CD8 T cells were shown not to accumulate in the inflamed liver (22). Recently, Geissmann et al. reported that CXCR6-deficient mice showed a reduction in NKT cell numbers in the liver and decreased susceptibility to Con A-induced hepatitis (23). In addition, blocking of the interaction between CXCL16 and CXCR6 by anti-CXCL16 mAb was shown to result in the failure to maintain graft tolerance (24).

In this study, we have further explored the physiological role of SR-PSOX/CXCL16 by generating and analyzing SR-PSOX/CXCL16-deficient mice. SR-PSOX-deficient mice showed not only a reduced number of liver NKT cells, but also severely and moderately impaired production of IFN-γ and IL-4, respectively, by administration of αGalCer. Moreover, *Propionibacterium acnes* (*P. acnes*)-induced Th1 responses were also impaired in both NKT-deficient and SR-PSOX-deficient mice. Taken together, SR-PSOX/CXCL16 was thus suggested to play a crucial role in not only the accumulation of liver NKT cells but also the enhancement of IFN-γ production by NKT cells, and the promotion of Th1-polarized immunological responses mediated by NKT cells.

Materials and Methods

Mutant Mice

SR-PSOX-deficient mice were generated in collaboration with Sankyo Co. Ltd. (Tokyo, Japan). Mouse genomic DNA containing the *SR-PSOX* gene was isolated from a mouse 129/SVJ genomic phage library (Stratagene). A targeting vector was constructed by replacing a genomic fragment containing exons 1, 2 and 3 with a DNA fragment containing a *neomycin resistance* gene (*neo*) (Fig. 1*A*). The targeting vector was introduced into ES cells (E14.1) by electroporation and the targeted clones were screened by Southern blot hybridization. SR-PSOX KO mice were backcrossed to C57BL6 mice for ten generations. All mice were bred and maintained in our animal facilities under specific pathogen-free conditions and examined at 6–12 wk of age. The genotyping of SR-PSOX KO mice was conducted by PCR using the following primers: 5′-taccgcagggtactttggatca-3′ and 5′-ttgcgctcaaagcagtccacta-3′, and 5′-ggatctcctgtcatctcaccttgc-3′ and 5′-cggc cacagtcgatgaatccagaa-3′ for detection of the wild-type SR-PSOX allele (151 bp) and knockout allele (333 bp), respectively. The lack of SR-PSOX expression at the RNA level was confirmed by RT-PCR using the primers, 5′-atgaggcggggctttggacccttg-3′ and 5′-agcaccggtacccaagctggtgtgc-3′ (614 bp). NKT cell-deficient mice (Vα14-deficient mouse) (25) were obtained from Research Center for Allergy and Immunology, RIKEN.

Reagents and antibodies

αGalCer (26) was kindly provided by Kirin Brewery Co. Ltd. (Takasaki, Japan). PE-labeled αGalCer/CD1d tetramer, prepared using a baculovirus expression system, was kindly provided by Dr M. Kronenberg (La Jolla Institute, La Jolla, CA). The following anti-mouse mAbs were purchased from BD Biosciences: anti-CD16/CD32 (2.4G2), anti-CD3 (2C11), anti-CD28 (37.51), PE-anti-NK1.1 (PK136), APC-anti-NK1.1, FITC-anti-TCRβ (H57–597), biotin-anti-TCRβ, APC-anti-TCRβ, biotin-anti-Ly49A (A1), PE-anti-CD11c (HL3) and FITC-anti-CD1d (1B1), FITC-anti-IFN-γ (XMG1.2) and PE-anti-IL-4 (BVD4-1D11). Neutralizing polyclonal anti-IL-4 was purchased from R & D. Anti-mouse SR-PSOX Ab (12–81) was generated by Sankyo Co Ltd. (Tokyo, Japan) as described previously (27).

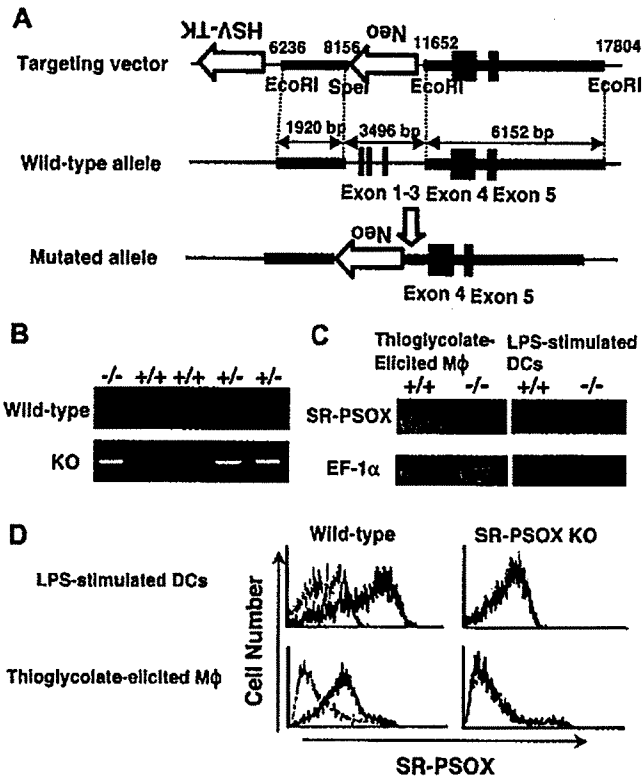

FIGURE 1. Generation of SR-PSOX/CXCL16-deficient mice. (*A*) Structure of the *SR-PSOX/CXCL16* genome (wild-type allele), the targeting vector and the predicted mutated *SR-PSOX/CXCL16* gene (Mutated allele). Filled boxes represent exons. The targeting vector was designed to replace the *Spe*I and *Eco*RI fragment containing exon 1, 2 and 3 of *SR-PSOX* with a *neomycin*-resistance gene (*Neo*). A Herpes simplex virus 1-thymidine kinase (HSV-TK) gene was ligated to the 5′ end of the targeting vector for negative selection. (*B*) PCR analysis of genomic DNA extracted from tails of SR-PSOX wild-type (+/+), heterozygous (+/−) and homozygous mutant (−/−) mice. The PCR product (151 bp) was amplified using wild-type SR-PSOX-specific primers (wild-type) from genomic DNA of the tails of the wild-type (+/+) and heterozygous (+/−) mice. The PCR product (333 bp) was amplified using knockout-specific primers (KO) from genomic DNA of the tails of the heterozygous (+/−) and homozygous (−/−) mice. (*C*) RT-PCR analysis of RNA extracted from thioglycolate-elicited macrophages and CD11c$^+$ DCs from the wild-type (+/+) and homozygous mutant (−/−) mice. Peritoneal thioglycolate-elicited macrophages were prepared from 4 days after i.p. injection of 4% thioglycolate. CD11c$^+$ DCs were prepared from spleen stimulated with LPS (1 μg/ml) for 2 days. Expression of SR-PSOX or translational elongation factor −1α (EF-1α) was examined by RT-PCR using total RNA from indicated cells. (*D*) Surface expression of SR-PSOX on thioglycolate-elicited macrophages and LPS-stimulated DCs. Flow cytometric analysis was conducted after staining with anti-SR-PSOX mAb (bold line) or control IgG (dotted line).

Recombinant IL-2, IL-12 and SR-PSOX/CXCL16 were purchased from Peprotech.

Preparation of leukocytes

Liver mononuclear cells were isolated as described previously (28, 29). In brief, the liver cell suspension was passed through stainless steel or nylon mesh, washed twice, re-suspended in a 33% percoll solution and centrifuged at 2,000 rpm for 10 min at room temperature. After lysing RBC, liver leukocytes were washed once and subjected to further analysis. CD11c$^+$ and NK1.1$^+$ cells were purified using MACS according to the manufacturer's directions (Miltenyi Biotec). NKT cells were further purified as CD3$^+$ and NK1.1$^+$ cells by using cell sorter, EPICS *Elite* (Coulter). Splenocyte and thymocyte suspensions were passed through nylon mesh and washed twice. After the lysing of RBC, cells were washed once and subjected to further analysis. Thioglycolate-elicited peritoneal macrophages were prepared from mice 4 days after i.p. injection of 4% thioglycolate (2 ml/mouse).

Flow cytometry

After blocking with anti-CD16/CD32 mAb for 15 min on ice, thymus, spleen or liver leukocytes were stained with various mAbs for 30 min on ice. For CXCR6 staining, murine CXCL16-human Fcγ fusion protein was used as described previously (15, 27). In brief, after blocking with anti-CD16/CD32 mAb, lymphocytes were incubated with CXCL16-Fcγ fusion protein or control human Fcγ for 30 min on ice, and the specific binding was detected by incubation with PE-conjugated anti-human Fcγ (Jackson ImmunoResearch) for 30 min on ice. For SR-PSOX/CXCL16 staining, isolated liver leukocytes were cultured for 2 h in RPMI 1640 medium containing 10% FBS, blocked with anti-CD16/CD32 mAb for 15 min on ice, and stained with PE-anti-CD11c, FITC-anti-CD1d and biotin-anti-SR-PSOX mAbs for 30 min on ice. Thereafter, cells were stained with streptavidin-PBXL for 30 min on ice, and then analyzed by flow cytometry using EPICS *Elite* (Coulter).

αGalCer stimulation

For in vivo αGalCer stimulation, serum was obtained from wild-type and SR-PSOX KO mice at the indicated time points after i.p. administration of αGalCer (100 μg/kg). For in vitro αGalCer stimulation, NKT and $CD11c^+$ liver cells were isolated from male wild-type and SR-PSOX KO mice. Then, the $CD11c^+$ APCs (2×10^4 cells/well) and the $CD3^+NK1.1^+$ NKT cells (2×10^4 cells/well) were stimulated with αGalCer (100 ng/ml) in 96-well U-bottom plates for 72 h. The culture supernatant and cells were collected for quantification of produced cytokines and apoptosis, respectively. The amounts of IFN-γ and IL-4 in the culture supernatant were determined using specific ELISA kits (R&D Systems, Minneapolis, MN) according to the manufacturer's instructions. For apoptosis detection assays, cells were stained with PE-anti-CD11c, followed by FITC-labeled Annexin-V according to the manufacturer's instructions (MBL) (24). After staining, cells were washed and analyzed by EPICS Elite (Coulter).

Quantitative RT-PCR analysis

Cells were directly lysed on TRIzol (Invitrogen) and total RNA was extracted following the manufacturer's instructions. Total cDNA was prepared using random primers (Promega Corporation) with PowerScript Reverse Transcriptase (Clontech) at 42°C for 90 min. The expression of T-bet and GATA-3 was analyzed by real time quantitative PCR using SYBR Green PCR Master Mix and ABI Prism 7500 Sequence Detection System (Applied Biosystems). Used primers were; T-bet, 5′-gttgacagttgggtcca ggt-3′ and 5′-cgccaggaagtttcatttgg-3′; GATA-3, 5′-tcggccattcgtacatggaa-3′ and 5′-gagagccgtggtggatggac-3′; GAPDH, 5′-ccttcattgacctcaacta-3′ and 5′-agtgatggcatggactgtggt-3′. The amounts of T-bet and GATA-3 in each sample were calculated with ABI Prism 7500 Sequence Detection System software (Applied Biosystems) and normalized to the amount of GAPDH.

Tumor growth assay

B16 melanoma cells (5×10^5 cells/mouse) was s.c. inoculated into male wild-type and SR-PSOX KO mice, and thereafter αGalCer (100 μg/kg) or vehicle was i.p. injected repeatedly at 4 days interval. Tumor volume was measured with a caliper every 2 days. Tumor volumes (mm^3) were calculated by the following formula: Tumor volumes (mm^3) = (longest diameter) × (shortest diameter) (2). The data shown represent the mean ± SEM.

Analysis of Th1 responses

To analyze in vitro cytokine-producing activity of Th1 cells generated in wild-type, SR-PSOX KO and NKT KO mice, $CD4^+$ T cells were isolated from these mice seven days after i.p. injection of heat-killed *P. acnes* (200 μg/mouse) using MACS CD4 T cells isolation kit. The isolated $CD4^+$ T cells, which were free of NKT cells, were then cultured in 2.5 μg/ml anti-CD3-coated plastic plates for 24 h, and culture supernatants were analyzed for IFN-γ and IL-4 production by ELISA. RNA from cell lysates were analyzed for T-bet and GATA-3 mRNA expression by real time quantitative RT-PCR. To analyze in vivo cytokine-producing activity of *P. acnes*–injected mice, LPS (1.5 μg/mouse) was administrated i.v. into wild-type, SR-PSOX KO and NKT NO mice seven days after i.v. injection of heat-killed *P. acnes* (250 μg/mouse). At the indicated time points after the administration of LPS, IFN-γ concentration and GPT activity in the serum were determined by ELISA and a GPT OA test Wako kit (Wako Pure Chemicals Industries), respectively.

In vitro generation of Th1 cells

For in vitro Th1 cell differentiation, $CD4^+$ naive T cells were isolated from spleen of male wild-type, SR-PSOX KO and NKT KO mice, and cultured in plastic plates coated with 2.5 μg/ml anti-CD3 mAb and 10 μg/ml anti-CD28 mAb in the presence of 4 ng/ml IL-2, 5 ng/ml IL-12 and 2.5 μg/ml neutralizing anti-IL-4 mAb for 7 days. Th1 differentiated CD4 T cells in wild-type, SR-PSOX KO and NKT KO mice were stained by anti-IFN-γ (XMG1.2) and anti-IL-4 Ab (BVD4-1D11) for intracellular cytokine staining.

Statistical Analysis

Statistical analyses between two groups were performed by two-sample *t* test. *p* values <0.05 were considered significant.

Results

Generation of SR-PSOX/CXCL16-deficient mice

To explore the role of SR-PSOX/CXCL16 in vivo, we generated SR-PSOX/CXCL16-deficient mice by replacing exon 1, 2, and 3 of the mouse *SR-PSOX* gene with a *neomycin-resistance* gene (Fig. 1*A*). The correct targeting of the SR-PSOX/CXCL16 locus was confirmed by genomic PCR analysis (Fig. 1*B*). SR-PSOX KO mice were born according to the expected Mendelian ratio when $SR\text{-}PSOX^{+/-}$ mice were intercrossed. SR-PSOX KO mice were fertile and macroscopically normal (data not shown). Because SR-PSOX/CXCL16 was described to be expressed on thioglycolate-elicited peritoneal macrophages or LPS-stimulated-$CD11c^+$ splenic DCs (15, 17), loss of SR-PSOX/CXCL16 expression was confirmed at both the RNA and protein level in these cells from SR-PSOX KO mice by RT-PCR and flow cytometry (Fig. 1*C* and *D*).

SR-PSOX plays an important role in αGalCer-induced IFN-γ production in vivo

αGalCer presented by CD1d on APCs is a specific ligand of NKT cells. αGalCer-stimulated NKT cells produce large amounts of both IFN-γ and IL-4, and the balance between the production of IFN-γ and IL-4 was reported to determine the type of immunological environment, Th1 or Th2 responses (2). CXCR6 was reported to be expressed on NKT cells and we confirm the expression of CXCR6 on liver NKT cells and the chemotactic and adhesion activity of SR-PSOX/CXCL16 against liver NKT cells (data not shown). To evaluate the contribution of SR-PSOX/CXCL16 to the activation of NKT cells by αGalCer in vivo, αGalCer was injected into wild-type and SR-PSOX KO mice, and serum levels of IFN-γ and IL-4 were quantified (Fig. 2*A*). In wild-type mice, serum IFN-γ levels were remarkably increased by the administration of αGalCer, peaked at 12 h and decreased to the basal level by 24 h. In contrast, the levels of IFN-γ in SR-PSOX KO mice were reduced to ~20% of those in wild-type mice. Serum IL-4 levels in wild-type mice also increased on administration of αGalCer, peaked at 3 h and decreased to the basal level by 6 h. The increased levels of serum IL-4 in SR-PSOX KO mice, however, were decreased to only 60% of those in wild-type mice. In SR-PSOX KO mice, the αGalCer-induced production of IFN-γ was more severely impaired than the production of IL-4.

αGalCer has been shown to exert an antitumor effect by inducing IFN-γ from NKT cells. In αGalCer-treated mice, s.c. tumor growth was reported to be inhibited in an IFN-γ dependent manner (5). To examine whether SR-PSOX is involved in in vivo antitumor effect of αGalCer, B16 melanoma cells were s.c. inoculated in wild-type and SR-PSOX KO mice and thereafter αGalCer was injected repeatedly. As reported previously, αGalCer treatment in wild-type mice significantly inhibited the outgrowth of s.c. inoculated B16 cells, while the anti-tumor effect was not observed in SR-PSOX KO mice (Fig. 2*B*). These results indicate that SR-PSOX/CXCL16 also plays an important role in IFN-γ production from αGalCer-treated NKT cells in vivo, which exerts a potent antitumor effect.

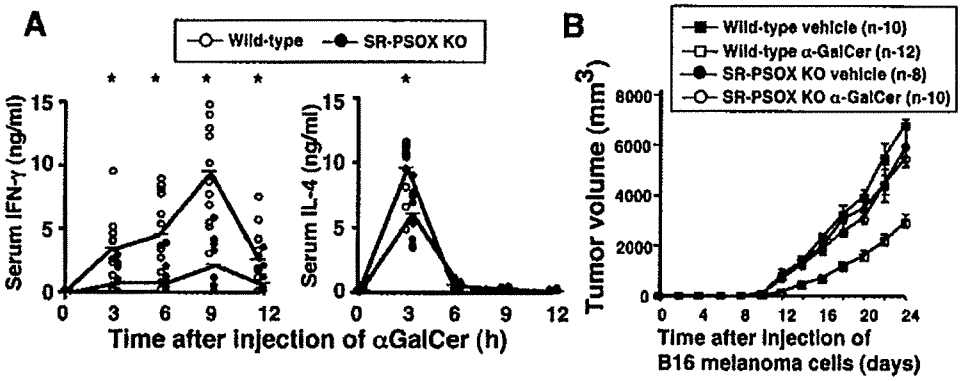

FIGURE 2. Requirement of SR-PSOX for IFN-γ production in αGalCer-administered mice. (*A*) Determination of serum levels of IFN-γ and IL-4 after i.p. injection of αGalCer. The amounts of serum IFN-γ and IL-4 were determined using specific ELISA kits (R&D Systems) in wild-type and SR-PSOX KO mice at the indicated time points after i.p. administration of αGalCer (100 μg/kg). Amounts of serum IFN-γ and IL-4 in vehicle-injected wild-type and SR-PSOX KO mice were under the detection limit. Statistical analysis was performed by two-sample *t* test between two groups, wild-type and SR-PSOX KO mice (*, $p < 0.05$). (*B*) In vivo antitumor effect of αGalCer. B16 melanoma cells (5×10^5 cells/mouse) were s.c. inoculated into male wild-type and SR-PSOX KO mice, and thereafter αGalCer or vehicle was injected repeatedly to wild-type and SR-PSOX KO mice at 4 days interval. Tumor volume was measured every 2 days. The data shown represent the mean ± SEM.

SR-PSOX/CXCL16 functions as a costimulatory factor to induce IFN-γ production by liver NKT cells

Recently, Geissmann et al. reported CXCR6 (a specific ligand for SR-PSOX/CXCL16)-deficient mice exhibit a selective reduction of the number of liver NKT cells (23). To examine the physiological roles of SR-PSOX/CXCL16 especially in regulation of the number and/or function of NKT cells in various organs, we examined the thymus, spleen and liver of SR-PSOX KO mice (Fig. 3). The absolute numbers of mononuclear cells in these organs of SR-PSOX KO mice were not significantly changed when compared with those of wild-type mice. Although the numbers of T ($NK1.1^-TCR\beta^+$) and NK cells ($NK1.1^+TCR\beta^-$) in these organs were essentially the same in SR-PSOX KO and wild-type mice, the number of liver NKT cells ($NK1.1^+TCR\beta^+$ and CD1d tetramers$^+TCR\beta^+$) was reduced in SR-PSOX KO mice compared with wild-type mice. The numbers of NKT cells in thymus and spleen of SR-PSOX KO mice were not decreased.

The impaired accumulation of liver NKT cells would be reflected by the overall reduction of αGalCer-induced production of cytokines including IFN-γ and IL-4, but cannot explain the greater defect in IFN-γ production compared with IL-4 production in αGalCer-administrated SR-PSOX KO mice. To examine the contribution of SR-PSOX to the production of cytokines by NKT cells in detail, we first investigated the expression of SR-PSOX in the liver. Because 1) SR-PSOX is expressed on activated APCs such as macrophages and DCs (Fig. 1*C* and *D*), 2) liver $CD11c^+$ cells were reported as liver DCs (30) and 3) CD1d is necessary for αGalCer to be presented to NKT cells, we investigated whether the expression of CD1d and CD11c is related to that of SR-PSOX/CXCL16. Liver $CD1d^+CD11c^+$ cells were found to express SR-PSOX/CXCL16 (Fig. 4*A*), while $CD1d^-CD11c^+$, $CD1d^+CD11c^-$ or $CD1d^-CD11c^-$ cells did not express it (data not shown). SR-PSOX/CXCL16 was thus shown to be expressed on liver APCs. Interestingly, cytofluorometric analyses revealed the expression of SR-PSOX to be increased by stimulation with αGalCer (Fig. 4*B*). We confirmed loss of SR-PSOX/CXCL16 expression in these $CD1d^+CD11c^+$ cells from SR-PSOX KO mice (Fig. 4*A*). In contrast, the numbers of $CD11c^+$ cells and $CD1d^+CD11c^+$ cells from the liver were shown to be almost equivalent between wild-type and SR-PSOX KO mice, and the costimulatory molecules CD80 and CD86 were equivalently expressed on $CD1d^+CD11c^+$ cells from SR-PSOX KO and wild-type mice (Fig. 4*A*). Thus, we did not detect any differences in the number and characteristics of liver DCs from wild-type and SR-PSOX KO mice without the expression of SR-PSOX.

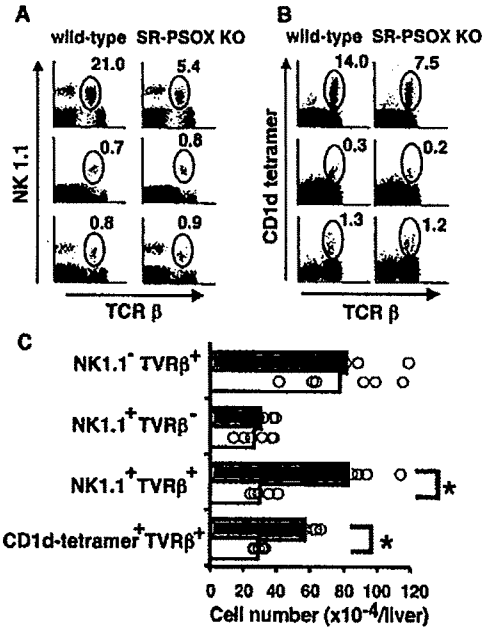

FIGURE 3. Characterization of NKT cells in the liver of SR-PSOX-deficient mice. (*A*) Quantification of NKT cells in the liver (upper), thymus (middle) and spleen (lower) from wild-type and SR-PSOX KO mice. Mononuclear cells were prepared from the indicated organs and stained with NK1.1 and TCRβ. The percentage of NKT cells ($NK1.1^+$ and TCR^+) among the mononuclear cells is shown. (*B*) Quantification of Vα14*i* NKT cells in the liver (upper), thymus (middle) and spleen (lower) from wild-type and SR-PSOX KO mice. Mononuclear cells were stained with CD1d-tetramer and TCRβ. In the case of splenocytes, cells were stained with CD1d-tetramer and TCRβ after B lymphocytes were eliminated. The percentage of Vα14*i* NKT cells among the mononuclear cells is shown. (*C*) Absolute numbers of T, NK and NKT cells in the liver of wild-type and SR-PSOX KO mice. Liver mononuclear cells were stained with NK1.1 and TCRβ. Absolute numbers of T ($NK1.1^-TCR\beta^+$), NK ($NK1.1^+TCR\beta^-$), NKT ($NK1.1^+TCR\beta^+$) and CD1d-tetramer$^+TCR\beta^+$ cells were determined by flow cytometry. Statistical analysis was performed by two-sample *t* test (*, $p < 0.05$).

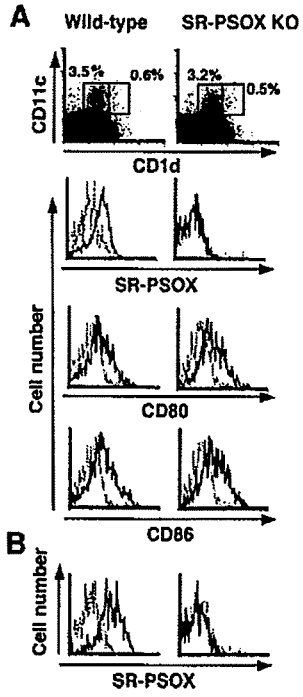

FIGURE 4. Expression of SR-PSOX/CXCL16 on liver $CD11c^+CD1d^+$ cells. (*A*) Surface expression of SR-PSOX, CD80 and CD86 on liver $CD11c^+CD1d^+$ cells. Mononuclear cells were isolated from the liver from wild-type or SR-PSOX KO mice, and stained with mAbs for CD11c, CD1d and SR-PSOX, CD80 or CD86. Upper panels: Total liver mononuclear cells were stained with CD11c and CD1d. $CD11c^+$ cells were 4.1 (3.5 + 0.6)% and 3.7 (3.2 + 0.5)% of total liver mononuclear cells from wild-type and SR-PSOX KO mice, respectively. $CD11c^+CD1d^+$ cells were 0.6% and 0.5% of total liver mononuclear cells from wild-type and SR-PSOX KO mice, respectively. Lower panels: Liver $CD11c^+CD1d^+$ cells were stained with anti-SR-PSOX mAb, CD80 or CD86. (*B*) Surface expression of SR-PSOX on liver $CD11c^+CD1d^+$ cells after in vitro cultivation with αGalCer. Mononuclear cells were isolated from the liver of wild-type or SR-PSOX KO mice, cultured in vitro for 48 h with αGalCer (100 ng/ml), and then stained with CD11c, CD1d and SR-PSOX. Histogram shows expression levels of SR-PSOX on liver $CD11c^+CD1d^+$ cells from wild-type and SR-PSOX KO mice.

To examine the contribution of SR-PSOX to the production of cytokine by NKT cells in detail, we next investigated α-GalCer-induced production of IFN-γ and IL-4 in vitro using total liver mononuclear cells isolated from wild-type and SR-PSOX KO mice. The liver leukocytes form wild-type mice stimulated with α-GalCer for 72 h showed vigorous production of IFN-γ and IL-4. In contrast, the liver leukocytes from SR-PSOX KO mice showed decreased production of both IFN-γ and IL-4 (Fig. 5*A*). These results would be caused by the decreased number of liver NKT cells in SR-PSOX KO mice compared with wild-type mice (Fig. 3). To examine the role of SR-PSOX/CXCL16 as a costimulatory factor, NKT cells were isolated from the liver of wild-type mice and cultured with isolated $CD11c^+$ cells from the liver of wild-type and SR-PSOX KO mice in the presence of αGalCer (100 ng/ml) for 72 h (Fig. 5*B*). αGalCer was clearly shown to induce production of IFN-γ and IL-4 by the NKT cells only when cocultured with $CD11c^+$ APCs from wild-type mice. Interestingly, the wild-type NKT cells, cocultured with SR-PSOX KO $CD11c^+$ APCs and stimulated with αGalCer, produced equal amounts of IL-4 but only about half the amount of IFN-γ as those cocultured with wild-type APC (Fig. 5*B*). In contrast, NKT cells from SR-PSOX KO mice were shown to be able to produce equivalent amounts of IFN-γ and IL-4 compared with wild-type NKT cells after cultivation with wild-type APC in the presence of αGalCer. We then examined the mRNA expression of T-bet (Th1-specific transcription factor) and GATA-3 (Th2-specific transcription factor) by quantitative real time RT-PCR. Wild-type NKT cells, cocultured with SR-PSOX KO $CD11c^+$ APCs and stimulated with αGalCer, showed similar amounts of GATA-3 mRNA expression and significantly reduced amounts of T-bet mRNA expression, compared with those cocultured with wild-type APC (Fig. 5*C*). NKT cells from SR-PSOX KO mice showed similar levels of GATA-3 and T-bet mRNA expressions by αGalCer stimulation.

Geissmann et al. demonstrated a deficiency of CXCR6 leading to reduced survival of NKT cells (23). We quantified apoptosis in liver NKT cells from wild-type and SR-PSOX-deficient mice after *in vitro* cultivation of liver mononuclear cells for 0, 7 and 14h, indicating that the numbers of annexin V-positive apoptotic NKT cells ($NK1.1^+TCR\beta^+$) to be the same in both groups (data not shown). We also quantified apoptosis in αGalCer-stimulated NKT cells. Purified liver NKT cells from wild-type or SR-PSOX KO mice were cultured with wild-type or SR-PSOX KO $CD11c^+$ APCs in the presence of αGalCer for 72h. Apoptotic NKT cells were then quantified as CD11c-negative and annexin-V-positive cells, indicating that the numbers of apoptotic NKT cells did not differ among all the groups (Fig. 5*D*). These results are not inconsistent with those of CXCR6-deficient mice, because the reduced survival of liver NKT cells in CXCR6-deficient mice was indicated to be independent of its ligand SR-PSOX/CXCL16 (23) and SR-PSOX-deficient NKT cells express CXCR6 (data not shown). Taken together, the reduced production of IFN-γ in SR-PSOX KO mice cannot simply explained by increased death of stimulated NKT cells, and SR-PSOX/CXCL16 was shown to function as a costimulatory factor for liver NKT cells expressing CXCR6 to produce IFN-γ but not IL-4. The costimulatory function of SR-PSOX may contribute the establishment of a Th1-polarized immune environment mediated by NKT- cells.

SR-PSOX-deficient mice are impaired in Propionibacterium acnes*–induced Th1 responses*

In several reports, IFN-γ production from NKT cells was shown to play important roles in host defense against bacteria (4). Expression of SR-PSOX/CXCL16 mRNA was reported to be increased in the mouse liver after administration of *Propionibacterium acnes* (*P. acnes*) (31), which is known to be an agent that induces Th1 responses in vivo (32, 33). Therefore, we examined *P. acnes*-induced Th1 responses in NKT-KO and SR-PSOX KO mice. After 7 days i.p. injection of heat-killed *P. acnes*, splenic CD4 T cells were isolated and stimulated with anti-CD3 mAb for 24 h. And then, culture supernatants were analyzed for IFN-γ and IL-4 production (Fig. 6*A*). Elevated production of IFN-γ, but not IL-4, was observed in *P. acnes*-primed wild-type CD4 T cells, however, *P. acnes*-primed CD4 T cells of NKT KO and SR-PSOX KO mice produced less than half the amounts of IFN-γ compared with those from wild-type mice (Fig. 6*A*). Of note, although CXCR6 was reported to be expressed on activated T cells prepared by in vitro cultivation with anti-CD3 and anti-CD28 (27), *P. acnes*-primed CD4 T cells did not express CXCR6 (data not shown), indicating that SR-PSOX on APCs and CXCR6 on NKT cells would play an important role in *P. acnes*-primed CD4 T cells to produce IFN-γ. We next examined the mRNA expression of T-bet and GATA-3 by quantitative real time RT-PCR. Although expression of T-bet mRNA, but not GATA-3 mRNA, was increased in *P. acnes*-primed wild-type CD4 T cells, *P. acnes*-primed CD4 T cells from NKT KO and SR-PSOX KO mice exhibited significantly lower T-bet expression than those from wild-type mice (Fig. 6*B*). We also analyzed serum IFN-γ level after administration of LPS into *P. acnes*-sensitized mice (Fig. 6*C*). Seven days after i.v. injection of heat-killed

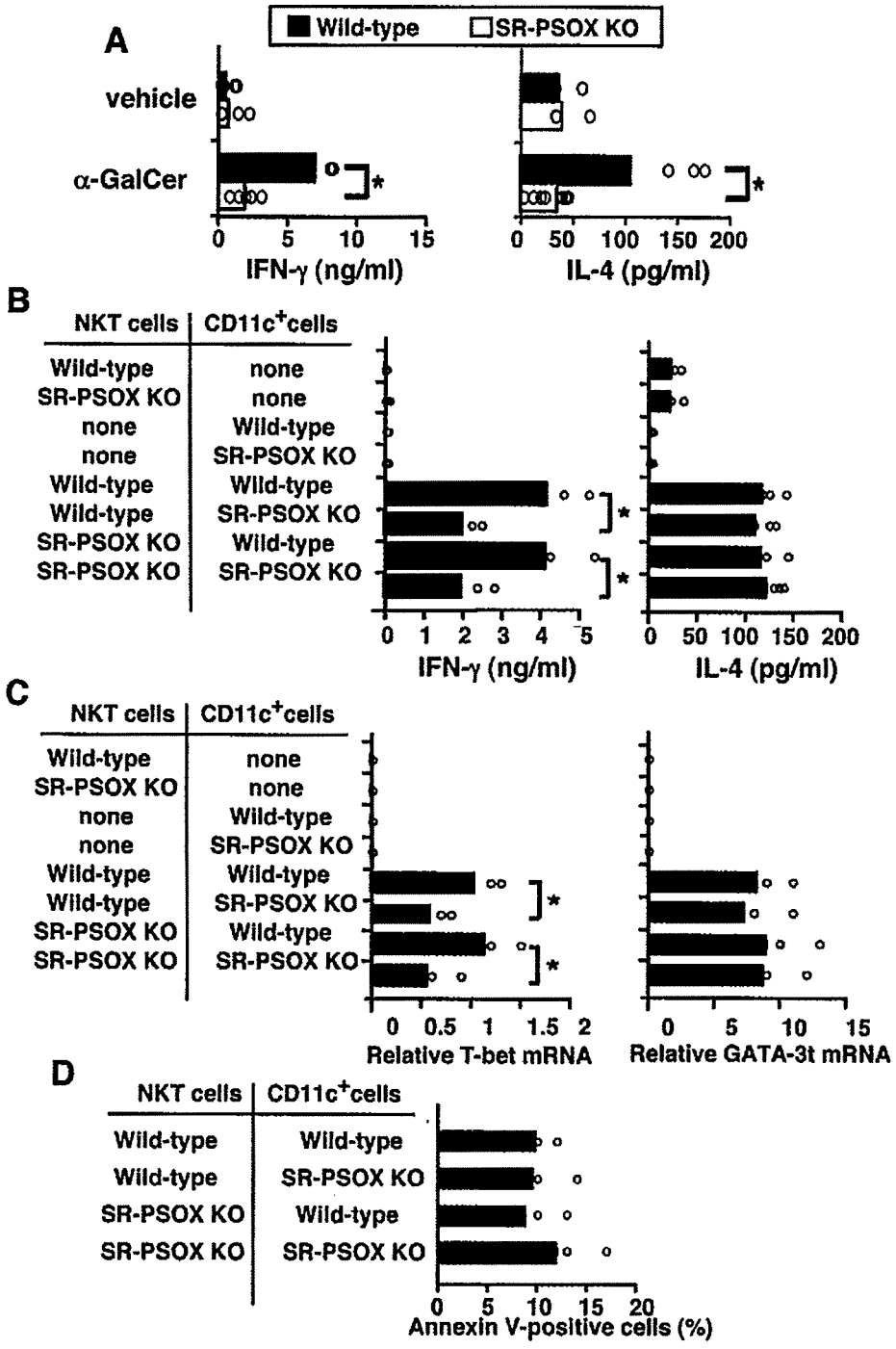

FIGURE 5. Costimulatory activity of SR-PSOX/CXCL16 to induce IFN-γ production by αGalCer-stimulated liver NKT cells. (*A*) αGalCer-induced in vitro responses in liver leukocytes. Freshly isolated liver leukocytes (2×10^5 cells/well) from male wild-type and SR-PSOX KO mice were stimulated with or without (vehicle) αGalCer (100 ng/ml) in 96-well U-bottom plates for 72 h. Then, the culture supernatant was collected and the amounts of IFN-γ and IL-4 in the culture supernatant were determined by ELISA. Statistical analysis was performed by two-sample *t* test (*, $p < 0.05$). (*B*) αGalCer-induced responses in reconstituted liver NKT and liver CD11c$^+$ APCs in vitro. CD3$^+$ and NK1.1$^+$ NKT cells and CD11c$^+$ liver cells were isolated from male wild-type and SR-PSOX KO mice. Then, the CD11c$^+$ APCs (2×10^4 cells/well) and the NKT cells (2×10^4 cells/well) were stimulated with αGalCer (100 ng/ml) in 96-well U-bottom plates for 72 h. Then, the culture supernatant was collected and the amounts of IFN-γ and IL-4 produced were determined by ELISA. Statistical analysis was performed by two-sample *t* test (*, $p < 0.05$). (*C*) αGalCer-induced responses in reconstituted liver NKT and liver CD11c$^+$ APCs in vitro. NKT and CD11c$^+$ liver cells were isolated as APCs from male wild-type and SR-PSOX KO mice. Then, the CD11c$^+$ APCs (2×10^4 cells/well) and the NKT cells (2×10^4 cells/well) were stimulated with αGalCer (100 ng/ml) in 96-well U-bottom plates for 72 h and isolated total RNA. Expression of T-bet and GATA-3 mRNA was determined by quantitative RT-PCR. The amount of each mRNA was normalized to GAPDH. Statistical analysis was performed by two-sample *t* test (*, $p < 0.05$). (*D*) αGalCer-induced apoptosis in liver NKT cocultured with liver CD11c$^+$ APCs in vitro. NKT and CD11c$^+$ liver cells were isolated from male wild-type and SR-PSOX KO mice. The CD11c$^+$ APCs (2×10^4 cells/well) and the NKT cells (2×10^4 cells/well) were cocultured and stimulated with αGalCer (100 ng/ml) for 72 h. Cells were collected and stained with PE-anti-CD11c and FITC-labeled Annexin-V. The numbers of apoptotic NKT cells were quantified as CD11c-negative and annexin-V-positive cells and expressed as percentages to the total number of CD11c-negative cells. Statistical analysis was performed by two-sample *t* test (*, $p < 0.05$).

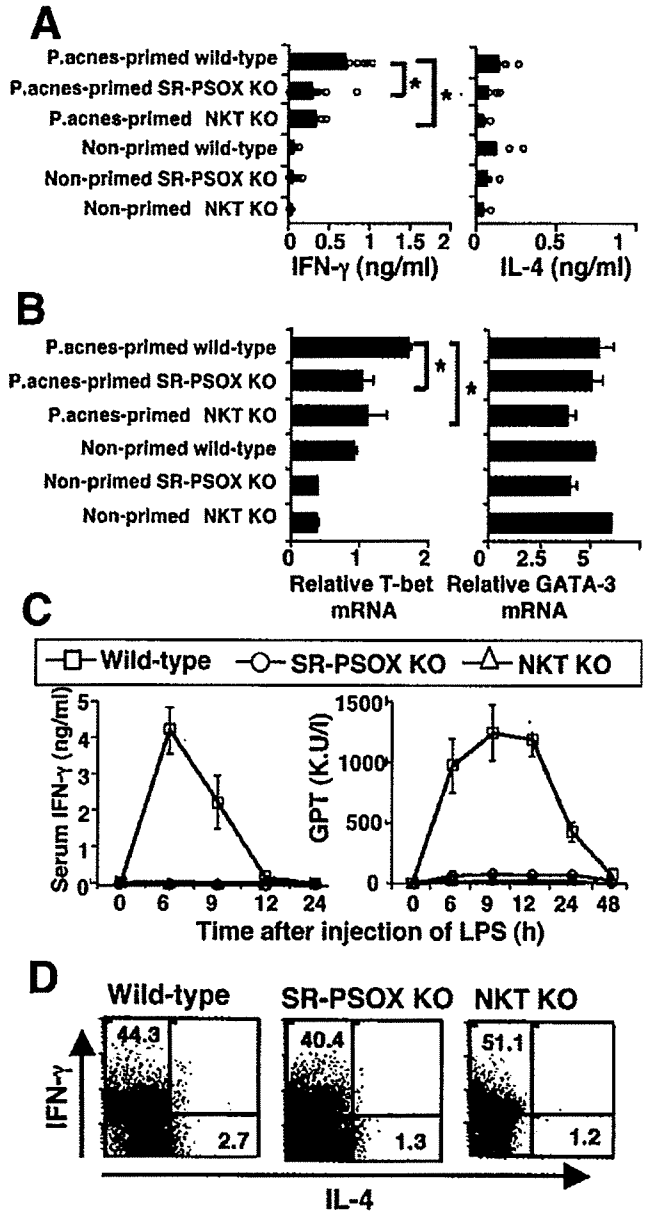

FIGURE 6. Impairment of in vivo Th1 responses in SR-PSOX KO and NKT KO mice. (*A*) Th1 responses induced by *P. acnes*. Male wild-type, SR-PSOX KO and NKT KO mice were i.p. injected with 200 μg/mouse heat-killed *P. acnes*. Seven days after injection, $CD4^+$ T cells from the spleen were stimulated with anti-CD3 for 24 h. Culture supernatants were analyzed for IFN-γ and IL-4 production by ELISA. Statistical analysis was performed by two-sample *t* test (*, $p < 0.05$). (*B*) Expression of T-bet and GATA-3 mRNA in *P. acnes*-primed $CD4^+$ T cells. Male wild-type, SR-PSOX KO and NKT KO mice were i.p. injected with 200 μg/mouse heat-killed *P. acnes*. Seven days after injection, $CD4^+$ T cells from the spleen were stimulated with anti-CD3 for 24h and isolated total RNA. Expression of T-bet and GATA-3 mRNA was determined by quantitative RT-PCR. The amount of each mRNA was normalized to GAPDH. Statistical analysis was performed by two-sample *t* test (*, $p < 0.05$). (*C*) LPS challenge in *P. acnes*-sensitized mice. Seven days after i.v. administration of heat-killed *P. acnes* (250 μg/mouse) into wild-type, SR-PSOX KO and NKT KO mice, 1.5 μg LPS was injected i.v. Serum IFN-γ concentration and GPT activity were determined at the indicated time points after the administration of LPS by ELISA and a GPT OA test Wako kit (Wako Pure Chemicals Industries), respectively. The data shown represent the mean ± SEM. (*D*) In vitro generation of Th1 cells from wild-type, SR-PSOX KO and NKT KO mice. Th1 cells were generated in Th1-skewed condition as described in *Materials and Methods*. Th1 differentiated CD4 T cells in wild-type, SR-PSOX KO and NKT KO mice were stained by anti-IFN-γ and anti-IL-4 Ab for intracellular cytokine staining.

P. acnes, small amount of LPS (1.5 μg/mouse) was i.v. injected. Serum IFN-γ levels were remarkably increased and peaked at 6 h after LPS injection in wild-type mice, whereas serum IFN-γ level was not increased in NKT-KO and SR-PSOX KO mice (Fig. 6*C*). The activity of GPT, a marker of damage to the liver, was also not increased in NKT KO and SR-PSOX KO mice (Fig. 6*C*). All the data show that both NKT cells and SR-PSOX/CXCL16 are involved in in vivo Th1 responses induced by *P. acnes*.

To confirm the role of NKT cell-induced cytokine in SR-PSOX/CXCL16-mediated in vivo Th1 responses, we further examined whether SR-PSOX/CXCL16 affected in vitro generation of Th1 cells in the absence of NKT cells. Splenic CD4 T cells from wild-type, NKT KO and SR-PSOX KO mice were cultured with anti-CD3 and anti-CD28 mAbs in the presence of IL-2, IL-12 and anti-IL-4 for 7 days, and then intracellular cytokine staining were performed. Significant differences were not found in IFN-γ and IL-4 production by in vitro generated Th1 cells from wild-type, NKT KO and SR-PSOX KO mice (Fig. 6*D*). Thus, SR-PSOX/CXCL16 and NKT cells were involved in neither in vitro generation of Th1 cells by cultivation with exogenous IL-2, IL-12 and anti-IL-4 nor production of IFN-γ from previously differentiated Th1 cells.

Discussion

In this study, αGalCer-administrated SR-PSOX KO mice showed severely and slightly impaired production of IFN-γ and IL-4, respectively (Fig. 2*A*). In SR-PSOX KO mice, the number of liver NKT cells was revealed to be specifically reduced (Fig. 3). This reduction in NKT cell numbers might be reflected by the overall reduced production of cytokines including IFN-γ and IL-4, but cannot fully explain the greater defect in IFN-γ production than IL-4 production in αGalCer-administrated SR-PSOX KO mice (Fig. 2*A*). We also demonstrated that SR-PSOX/CXCL16 is expressed on $CD1d^+CD11c^+$ cells and functions as a costimulatory factor to induce liver NKT cells to produce IFN-γ but not IL-4 through reduction of T-bet mRNA expression (Th1-specific transcription factor) (Fig. 5). Taken together, severe impairments of αGalCer-induced IFN-γ production in SR-PSOX KO mice in vivo would be reflected by both reduction of the number of liver NKT cells and defect of the costimulatory function of APCs to induce IFN-γ from NKT cells. We also investigated IFN-γ production by NKT cells in SR-PSOX KO and wild-type mice after stimulation with iGb3, a commercially available physiological ligand for NKT cells; however significant amounts of IFN-γ were not detected in either serum of iGb3-injected mice nor culture supernatant of iGb3-stimulated total liver leukocytes (data not shown).

NKT cells produce large amounts of IFN-γ and/or IL-4 soon after stimulation with αGalCer, and regulate the development of Th1 and Th2 cells (2). CD40, CD28 and LFA-1 on APC are reported to work as costimulatory factors in IFN-γ and/or IL-4 production by αGalCer-stimulated NKT cells (11, 12). CD40 mediates production of IFN-γ but not of IL-4, while CD28 is important for both (11). Interestingly, in αGalCer administrated LFA-1-deficient mice, the production of IL-4 was increased twice as compared with wild-type, although the production of IFN-γ was almost normal (12). GATA-3 expression but not T-bet was increased in LFA-deficient NKT cells by in vitro αGalCer-stimulation. In contrast, our data indicate that T-bet expression in NKT cells is important for SR-PSOX-induced IFN-γ production. Taken together, LFA-1 acts as a negative regulator of NKT cell-regulated Th2-like immunity induced by αGalCer, while SR-PSOX acts as a positive regulator of NKT cell-regulated Th1-like immunity by αGalCer (12). LFA-1-deficient mice also show a reduction in the number of NKT cells only in the liver. Given that chemokines presented on endothelial cells are known to mediate the activation of integrin,

and both chemokine and integrin are necessary for leukocytes to be arrested in the secondary lymphoid organs (13, 14), SR-PSOX and LFA-1 may play an important role not only in the control of the liver-specific accumulation of NKT cells but also in the regulation of IFN-γ and IL-4 production as costimulatory molecules.

CXCR6 was shown to be expressed on IFN-γ-producing Th1 cells as well as NKT cells (15, 16, 18, 20), and Th1 cells generated in vitro also showed chemotaxis and adhesion activities toward SR-PSOX/CXCL16 (data not shown). We also found severely impaired *P. acnes*-induced in vivo Th1 response in NKT KO and SR-PSOX KO mice (Fig. 6*A–C*). However, Th1 cells from splenocytes and in vitro stimulated Th1 cells were normal in both NKT KO and SR-PSOX KO mice (Fig. 6*D*). All these results indicate that SR-PSOX/CXCL16 is involved in *P. acnes*-induced Th1 response by stimulating NKT cells to produce IFN-γ, likely by acting as a costimulatory molecule. However, it remains to be determined how NKT cells and their produced IFN-γ induce in vivo generation of Th1 cells by *P. acnes* administration.

In conclusion, SR-PSOX plays a crucial role in in vivo IFN-γ production by administration of αGalCer and SR-PSOX on liver $CD11c^+CD1d^+$ dendritic cells enhances in vitro IFN-γ production from NKT cells as a costimulatory factor. SR-PSOX also plays important roles in inducing Th1 responses in vivo. Potent cytokine producing activity of NKT cells by αGalCer stimulation has been recognized to be an attractive target for various immunotherapies, because regulation of NKT cell-produced cytokine (IFN-γ or IL-4) has been shown to control Th1- or Th2-inclined immune responses involved in infection immunity, anti-tumor immunity, autoimmune disease and tolerance (1, 2, 20, 21, 34). Importantly, activation of NKT cells was reported to protect NOD mice and other mice from the onset and recurrence of autoimmune type I diabetes (7–9) and the onset of EAE (10), respectively, by suppressing IFN-γ production and/or enhancing IL-4 production. Modification of SR-PSOX-stimulated IFN-γ production from NKT cells may be useful in stimulation or suppression of NKT cell-mediated immunotherapy as well as immune reactions.

Acknowledgment

We thank Drs. K. Sakamaki, K. K. Lee, O. Yoshie, S. Ueha, K. Matsuno, and M. Harada for generous help.

Disclosures

The authors have no financial conflict of interest.

References

1. Seino, K., and M. Taniguchi. 2004. Functional roles of NKT cell in the immune system. *Front Biosci.* 9: 2577–2587.
2. Kronenberg, M. 2005. Toward an understanding of NKT cell biology: progress and paradoxes. *Annu. Rev. Immunol.* 23: 877–900.
3. Van Kaer, L. 2005. α-Galactosylceramide therapy for autoimmune diseases: prospects and obstacles. *Nat. Rev. Immunol.* 5: 31–42.
4. Kronenberg, M., and L. Gapin. 2002. The unconventional lifestyle of NKT cells. *Nat. Rev. Immunol.* 2: 557–568.
5. Hayakawa, Y., K. Takeda, H. Yagita, M. J. Smyth, L. Van Kaer, K. Okumura, and I. Saiki. 2002. IFN-γ-mediated inhibition of tumor angiogenesis by natural killer T-cell ligand, α-galactosylceramide. *Blood* 100: 1728–1733.
6. Seino, K., S. Fujii, M. Harada, S. Motohashi, T. Nakayama, T. Fujisawa, and M. Taniguchi. 2005. Vα14 NKT cell-mediated anti-tumor responses and their clinical application. *Springer Semin. Immunopathol.* 27: 65–74.
7. Sharif, S., G. A. Arreaza, P. Zucker, Q. S. Mi, J. Sondhi, O. V. Naidenko, M. Kronenberg, Y. Koezuka, T. L. Delovitch, J. M. Gombert, et al. 2001. Activation of natural killer T cells by α-galactosylceramide treatment prevents the onset and recurrence of autoimmune Type 1 diabetes. *Nat. Med.* 7: 1057–1062.
8. Hong, S., M. T. Wilson, I. Serizawa, L. Wu, N. Singh, O. V. Naidenko, T. Miura, T. Haba, D. C. Scherer, J. Wei, M. Kronenberg, Y. Koezuka, and L. Van Kaer. 2001. The natural killer T-cell ligand α-galactosylceramide prevents autoimmune diabetes in non-obese diabetic mice. *Nat. Med.* 7: 1052–1056.
9. Hammond, K. J., L. D. Poulton, L. J. Palmisano, P. A. Silveira, D. I. Godfrey, and A. G. Baxter. 1998. α/β-T cell receptor $(TCR)^+CD4^-CD8^-$ (NKT) thymocytes prevent insulin-dependent diabetes mellitus in nonobese diabetic (NOD)/Lt mice by the influence of interleukin (IL)-4 and/or IL-10. *J. Exp. Med.* 187: 1047–1056.
10. Miyamoto, K., S. Miyake, and T. Yamamura. 2001. A synthetic glycolipid prevents autoimmune encephalomyelitis by inducing TH2 bias of natural killer T cells. *Nature* 413: 531–534.
11. Hayakawa, Y., K. Takeda, H. Yagita, L. Van Kaer, I. Saiki, and K. Okumura. 2001. Differential regulation of Th1 and Th2 functions of NKT cells by CD28 and CD40 costimulatory pathways. *J. Immunol.* 166: 6012–6018.
12. Matsumoto, G., E. Kubota, Y. Omi, U. Lee, and J. M. Penninger. 2004. Essential role of LFA-1 in activating Th2-like responses by α-galactosylceramide-activated NKT cells. *J. Immunol.* 173: 4976–4984.
13. Moser, B., and P. Loetscher. 2001. Lymphocyte traffic control by chemokines. *Nat Immunol.* 2: 123–128.
14. Cyster, J. G. 2005. Chemokines, sphingosine-1-phosphate, and cell migration in secondary lymphoid organs. *Annu. Rev. Immunol.* 23: 127–159.
15. Matloubian, M., A. David, S. Engel, J. E. Ryan, and J. G. Cyster. 2000. A transmembrane CXC chemokine is a ligand for HIV-coreceptor Bonzo. *Nat. Immunol.* 1: 298–304.
16. Wilbanks, A., S. C. Zondlo, K. Murphy, S. Mak, D. Soler, P. Langdon, D. P. Andrew, L. Wu, and M. Briskin. 2001. Expression cloning of the STRL33/BONZO/TYMSTRligand reveals elements of CC, CXC, and CX3C chemokines. *J. Immunol.* 166: 5145–5154.
17. Shimaoka, T., N. Kume, M. Minami, K. Hayashida, H. Kataoka, T. Kita, and S. Yonehara. 2000. Molecular cloning of a novel scavenger receptor for oxidized low density lipoprotein, SR-PSOX, on macrophages. *J. Biol. Chem.* 275: 40663–40666.
18. Shimaoka, T., T. Nakayama, N. Kume, S. Takahashi, J. Yamaguchi, M. Minami, K. Hayashida, T. Kita, J. Ohsumi, O. Yoshie, and S. Yonehara. 2003. Cutting edge: SR-PSOX/CXC chemokine ligand 16 mediates bacterial phagocytosis by APCs through its chemokine domain. *J. Immunol.* 171: 1647–1651.
19. Tabata, S., N. Kadowaki, T. Kitawaki, T. Shimaoka, S. Yonehara, O. Yoshie, and T. Uchiyama. 2005. Distribution and kinetics of SR-PSOX/CXCL16 and CXCR6 expression on human dendritic cell subsets and $CD4^+$ T cells. *J. Leukocyte Biol.* 77: 777–786.
20. Kim, C. H., E. J. Kunkel, J. Boisvert, B. Johnston, J. J. Campbell, M. C. Genovese, H. B. Greenberg, and E. C. Butcher. 2001. Bonzo/CXCR6 expression defines type 1-polarized T-cell subsets with extralymphoid tissue homing potential. *J. Clin. Invest.* 107: 595–601.
21. Fukumoto, N., T. Shimaoka, H. Fujimura, S. Sakoda, M. Tanaka, T. Kita, and S. Yonehara. 2004. Critical roles of CXC chemokine ligand 16/scavenger receptor that binds phosphatidylserine and oxidized lipoprotein in the pathogenesis of both acute and adoptive transfer experimental autoimmune encephalomyelitis. *J. Immunol.* 173: 1620–1627.
22. Sato, T., H. Thorlacius, B. Johnston, T. L. Staton, W. Xiang, D. R. Littman, and E. C. Butcher. 2005. Role for CXCR6 in recruitment of activated $CD8^+$ lymphocytes to inflamed liver. *J. Immunol.* 174: 277–283.
23. Geissmann, F., T. O. Cameron, S. Sidobre, N. Manlongat, M. Kronenberg, M. J. Briskin, M. L. Dustin, and D. R. Littman. 2005. Intravascular immune surveillance by $CXCR6^+$ NKT cells patrolling liver sinusoids. *PLoS Biol.* 3: e113.
24. Jiang, X., T. Shimaoka, S. Kojo, M. Harada, H. Watarai, H. Wakao, N. Ohkohchi, S. Yonehara, M. Taniguchi, and K. Seino. 2005. Cutting edge: critical role of CXCL16/CXCR6 in NKT cell trafficking in allograft tolerance. *J. Immunol.* 175: 2051–2055.
25. Cui, J., T. Shin, T. Kawano, H. Sato, E. Kondo, I. Toura, Y. Kaneko, H. Koseki, M. Kanno, and M. Taniguchi. 1997. Requirement for Vα14 NKT cells in IL-12-mediated rejection of tumors. *Science* 278: 1623–1626.
26. Kawano, T., J. Cui, Y. Koezuka, I. Toura, Y. Kaneko, K. Motoki, H. Ueno, R. Nakagawa, H. Sato, E. Kondo, et al. 1997. CD1d-restricted and TCR-mediated activation of Vα14 NKT cells by glycosylceramides. *Science* 278: 1626–1629.
27. Shimaoka, T., T. Nakayama, N. Fukumoto, N. Kume, S. Takahashi, J. Yamaguchi, M. Minami, K. Hayashida, T. Kita, J. Ohsumi, et al. 2004. Cell surface-anchored SR-PSOX/CXC chemokine ligand 16 mediates firm adhesion of CXC chemokine receptor 6-expressing cells. *J. Leukocyte Biol.* 75: 267–274.
28. Goossens, P. L., H. Jouin, G. Marchal, and G. Milon. 1990. Isolation and flow cytometric analysis of the free lymphomyeloid cells present in murine liver. *J. Immunol. Methods* 132: 137–144.
29. Watanabe, H., K. Ohtsuka, M. Kimura, Y. Ikarashi, K. Ohmori, A. Kusumi, T. Ohteki, S. Seki, and T. Abo. 1992. Details of an isolation method for hepatic lymphocytes in mice. *J. Immunol. Methods* 146: 145–154.
30. Trobonjaca, Z., F. Leithauser, P. Moller, R. Schirmbeck, and J. Reimann. 2001. Activating immunity in the liver, I: liver dendritic cells (but not hepatocytes) are potent activators of IFN-γ release by liver NKT cells. *J. Immunol.* 167: 1413–1422.
31. Dong, H., N. Toyoda, H. Yoneyama, M. Kurachi, T. Kasahara, Y. Kobayashi, H. Inadera, S. Hashimoto, and K. Matsushima. 2002. Gene expression profile analysis of the mouse liver during bacteria-induced fulminant hepatitis by a cDNA microarray system. *Biochem. Biophys. Res. Commun.* 298: 675–686.
32. Okamura, H., K. Kawaguchi, K. Shoji, and Y. Kawade. 1982. High-level induction of γ interferon with various mitogens in mice pretreated with Propionibacterium acnes. *Infect. Immun.* 38: 440–443.
33. Matsui, K., T. Yoshimoto, H. Tsutsui, Y. Hyodo, N. Hayashi, K. Hiroishi, N. Kawada, H. Okamura, K. Nakanishi, and K. Higashino. 1997. Propionibacterium acnes treatment diminishes $CD4^+$ $NK1.1^+$ T cells but induces type I T cells in the liver by induction of IL-12 and IL-18 production from Kupffer cells. *J. Immunol.* 159: 97–106.
34. Zhou, D., J. Mattner, C. Cantu III, N. Schrantz, N. Yin, Y. Gao, Y. Sagiv, K. Hudspeth, Y. P. Wu, T. Yamashita, et al. 2004. Lysosomal glycosphingolipid recognition by NKT cells. *Science* 306: 1786–1789.

Available online at www.sciencedirect.com
ScienceDirect
Journal of Molecular and Cellular Cardiology 44 (2008) 76–83
Journal of Molecular and Cellular Cardiology
www.elsevier.com/locate/yjmcc

Original article

LOX-1 abrogation reduces myocardial ischemia–reperfusion injury in mice

Changping Hu [a,b], Jiawei Chen [a], Abhijit Dandapat [a], Yoshiko Fujita [c], Nobutaka Inoue [c], Yosuke Kawase [d], Kou-ichi Jishage [d], Hiroshi Suzuki [d,e], Dayuan Li [a], Paul L. Hermonat [a], Tatsuya Sawamura [a,f], Jawahar L. Mehta [a,*]

[a] *Department of Internal Medicine, University of Arkansas for Medical Sciences and Central Arkansas Veterans Healthcare System, Little Rock, AR, USA*
[b] *Department of Pharmacology, School of Pharmaceutical Sciences, Central South University, Changsha, China*
[c] *Department of Vascular Physiology, National Cardiovascular Center Research Institute, Osaka, Japan*
[d] *Chugai Research Institute for Medical Science, Inc., Japan*
[e] *Research Unit for Functional Genomics, National Research Center for Protozoan Diseases, Obihiro University of Agriculture and Veterinary Medicine, Obihiro, Hokkaido, Japan*
[f] *Department of Developmental and Medical Technology, Graduate School of Medicine, University of Tokyo, Tokyo, Japan*

Received 21 September 2007; accepted 12 October 2007
Available online 23 October 2007

Abstract

LOX-1 is a newly described lectin-like receptor for oxidized-LDL (ox-LDL), which is over-expressed in the ischemic myocardium. To examine the pathogenic role of LOX-1 in the determination of ischemia–reperfusion (I–R) injury to the heart, we developed LOX-1 knockout (KO) mice, and subjected these mice to 60 min of left coronary artery occlusion followed by 60 min of reperfusion. I–R in the LOX-1 KO mice resulted in a significant reduction in myocardial injury as well as in accumulation of inflammatory cells in the I–R myocardium and lipid peroxidation ($P<0.01$ vs. wild-type mice). Concomitantly, there was significant preservation of cardiac function in the LOX-1 KO mice despite I–R ($P<0.01$ vs. the wild-type mice). The phosphorylation of oxidative stress-sensitive mitogen-activated protein kinase (p38MAPK) and protein kinase B/Akt-1, expression of nitrotyrosine and inducible nitric oxide synthase (iNOS), and superoxide dismutase activity were enhanced during I–R in the wild-type mice. These alterations in p38MAPK, Akt-1 and iNOS were much less pronounced in the LOX-1 KO mice. The superoxide dismutase activity increased further in the LOX-1 KO mice. These observations provide compelling evidence that LOX-1 may be a key modulator of myocardial I–R injury, and its effect is mediated by pro-oxidant signals. LOX-1 may be a potential target for therapy of myocardial ischemic injury.

Keywords: LOX-1; Ischemia–reperfusion; Mitogen-activated protein kinase; Protein kinase B/Akt-1; Inducible nitric oxide synthase

1. Introduction

Ischemic myocardium is characterized by oxidative stress (release of reactive oxygen species [ROS]), inflammation and cell injury [1]. ROS are released in the early stages of ischemia–reperfusion (I–R) and act as chemoattractants for inflammatory cells; together they induce cell injury. ROS can oxidize low-density lipoproteins (LDL) [2], and the oxidized-LDL (ox-LDL) can injure cell membranes [3], further stimulate ROS generation [4] and increase inducible nitric oxide synthase (iNOS) expression [5], all part and parcel of I–R injury. Actually, perfusion of isolated hearts with ox-LDL *per se* results in myocardial injury [6]. Further, plasma levels of soluble ox-LDL are markedly elevated in patients with acute coronary syndromes [7], and the ischemic tissues contain large amounts of ox-LDL [8].

LOX-1, a lectin-like receptor for ox-LDL, was identified primarily on endothelial cells [9–11]. LOX-1 binds to and internalizes ox-LDL [9]. LOX-1 is upregulated by ROS, and itself stimulates the formation of ROS [10,11]. Its activation leads to

Abbreviations: iNOS, inducible nitric oxide synthase; I–R, ischemia–reperfusion; KO, knockout; LOX-1, a lectin-like receptor for oxidized low-density lipoprotein; MAPK, mitogen-activated protein kinase; NF-κB, nuclear factor-kappa B; NO, nitric oxide; ox-LDL, oxidized low-density lipoprotein; ROS, reactive oxygen species.

* Corresponding author. Division of Cardiovascular Medicine, University of Arkansas for Medical Sciences, 4301 West Markham St., Slot 532, Little Rock, AR 72205-7199, USA. Tel.: +1 501 296 1401; fax: +1 501 686 8319.
E-mail address: MehtaJL@uams.edu (J.L. Mehta).

0022-2828/$ - see front matter © 2007 Elsevier Inc. All rights reserved.
doi:10.1016/j.yjmcc.2007.10.009

activation of intracellular signaling involving oxidative stress-sensitive mitogen-activated protein kinases (MAPKs) and nuclear factor-kappa B (NF-κB) leading to inflammatory phenotype of the cells and apoptosis [11,12]. Our previous studies showed that LOX-1 is over-expressed in ischemic myocardium and treatment of rats with a specific antibody to LOX-1 before ischemia can prevent myocardial I–R injury [13,14]. Interestingly, plasma levels of soluble LOX-1 are elevated in patients with acute coronary syndrome [15]. These observations collectively suggest that LOX-1 may be an important player in myocardial I–R injury.

In order to conclusively determine the pathogenic role of LOX-1 in I–R injury, we engineered LOX-1 knockout (KO) mice [16]. Our findings in this animal model reveal that "taking away" LOX-1 expression limits myocardial I–R injury.

2. Materials and methods

2.1. Animals

C57BL/6 mice (also referred to as wild-type mice) were originally obtained from Jackson Laboratories. The homozygous LOX-1 KO mice were developed as described recently [16], and backcrossed 8 times with C57BL/6 strain to replace the genetic background. Male mice were utilized at 8–10 weeks of age (body weight: 20–24 g). All animals received humane care in compliance with the Public Health Service Policy on Humane Care and Use of Laboratory Animals published by NIH. The LOX-1 genotypes were verified as described recently [16].

2.2. RT–PCR analysis of LOX-1 expression

LOX-1 expression was analyzed by RT–PCR as described recently [16].

2.3. Immunohistochemical staining

5-μm-thick heart sections were incubated with primary antibody to mouse LOX-1 (3.5 μg/mL) overnight at 4 °C, rinsed with PBS, and incubated with biotinylated secondary antibody for 30 min. The slides were then incubated in avidin–biotin complex for 30 min followed by rinsing with PBS, and then incubated in diaminobenzidine and finally washed in distilled water and counterstained with hematoxylin. To confirm the presence of endothelium, heart sections were incubated with the anti-mouse CD31 antibody (Pharmingen) for 1 h at room temperature.

2.4. Myocardial ischemia–reperfusion protocol

Animals were anesthetized with sodium pentobarbital (60 mg/kg, i.p.) and mechanically ventilated with room air (tidal volume 1.4 ml, rate 110 strokes/min). Electrocardiogram (ECG) was continuously monitored throughout the experiment.

After an equilibration period of 10 min, left thoracotomy was performed in the fourth intercostal space and the pericardium was opened to expose the heart. A 6-0 silk suture was passed around the left coronary artery at a point two thirds of the way between its origin near the pulmonary conus and the cardiac apex. Sustained coronary artery occlusion achieved by clamping the snare against the surface of the heart caused an area of epicardial cyanosis with regional hypokinesia and ECG changes. Reperfusion was confirmed by hyperemic blushing of the previously ischemic myocardium. All mice were subjected to 60 min of coronary artery occlusion followed by 60 min of reperfusion, except the sham groups of animals that underwent the same procedure but without ligation of the coronary artery. The experimental procedures were approved by the Institutional Animal Care and Usage Committee.

2.5. Assessment of left ventricular hemodynamics

A 1.4-Fr Millar (SPR-671) pressure catheter was inserted through the right carotid artery into the left ventricle (LV). Analog inputs from the pressure transducer were amplified using a Bridge amplifier and digitized with a PowerLab data-acquisition system (AD Instruments). Heart rate (HR) and LV developed pressure (LVDP) were calculated from at least 30 consecutive beats. The first derivatives of the pressure over time ($\pm dP/dt_{max}$) were calculated from LV pressure tracings.

2.6. Determination of infarct size and myocardial injury

At the end of reperfusion, the left coronary artery was re-occluded, and 1 ml of 1% Evans blue was injected into the LV cavity and allowed to perfuse the non-ischemic portions of the heart. The entire heart was rinsed of excess blue dye, trimmed of right ventricular and atrial tissues, and sliced into 1-mm-thick sections. The slices were incubated in 1% triphenyl tetrazolium chloride (Sigma) at 37 °C for 15 min to stain the viable myocardium. The slices were then fixed in 10% formalin solution for 24 h, then imaged with planimetry (NIH Image J 1.34s) and following parameters analyzed: (a) area at risk (AAR) as a percent of total LV (AAR/LV), (b) the infarct area (IA) as a percent of AAR (IA/AAR), and (c) IA as percent of total LV (IA/LV).

In some experiments, hearts were embedded in paraffin and cut into 5-μm-thick sections. The sections were stained with either H&E or Masson's trichrome. Staining with trichrome delineates the injured regions. The sections were examined by a pathologist who independently evaluated the extent of myocardial injury and inflammatory cell infiltration.

2.7. Determination of serum creatine kinase-MB and MDA

At the end of reperfusion, blood was collected. Serum levels of creatine kinase-MB and MDA were measured spectrophotometrically according to the manufacture's instructions. Creatine kinase-MB and MDA kits were obtained from Stanbio Laboratory and Oxis International, respectively.

2.8. Superoxide Dismutase (SOD) Activity

Mice heart homogenates were cleared by centrifugation at 15,000×*g* for 30 min at 4 °C, and supernatants were used for measurements of Cu/Zn SOD activity as described previously [16].

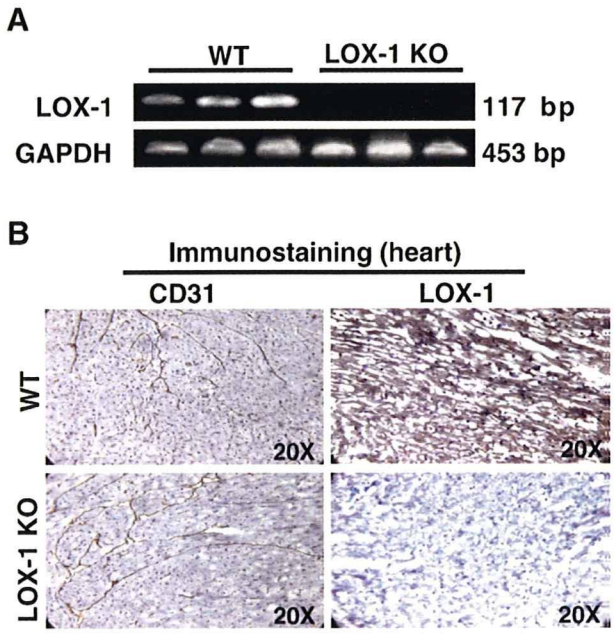

Fig. 1. Confirmation of LOX-1 deletion. The absence of LOX-1 expression in the LOX-1 knockout (KO) mice was analyzed by RT–PCR (A) and immunohistochemical staining (B). WT: wild-type.

2.9. Protein expression analysis

The entire LV was isolated for the Western analysis of LOX-1, nitrotyrosine, MAPKs (p38 and p44/42), Akt-1 and iNOS [15]. The relative intensities of protein bands were normalized to α-tubulin signal.

2.10. Statistical analysis

Data are expressed as mean±SE. The between-group difference in the infarct size was evaluated by unpaired *t*-test. Hemodynamic parameters were measured at indicated time-points repeatedly and analyzed with a two-way ANOVA with repeated measures; all other data were analyzed by a two-way ANOVA with Bonferroni post-hoc test. A P value of less than 0.05 was considered to be significant.

3. Results

3.1. Confirmation of LOX-1 deletion

Lack of LOX-1 expression in LOX-1 KO mice was confirmed by RT–PCR analysis of aortic tissues (Fig. 1A). LOX-1 expression was not detected in LOX-1 KO mice heart, although the presence of endothelium was confirmed by simultaneous staining of CD31, a marker of endothelial cells. The LOX-1 expression was clearly detectable in the wild-type mice (Fig. 1B).

3.2. Ischemia–reperfusion and expression of LOX-1 in the heart

In keeping with previous studies [13,14], LOX-1 expression was increased during I–R in the hearts of wild-type mice. The

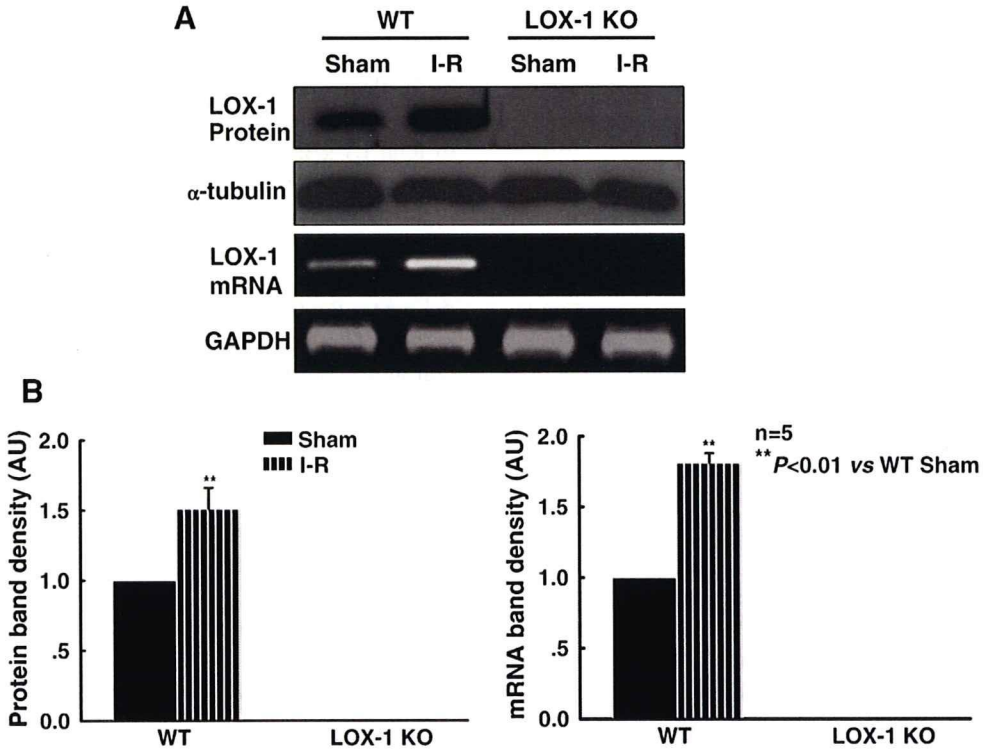

Fig. 2. LOX-1 expression in the myocardium. LOX-1 expression was determined by RT–PCR and Western analysis. KO: knockout; I–R: ischemia–reperfusion; WT: wild-type.

LOX-1 KO mice, as expected, did not show LOX-1 despite the same degree of I–R as in the wild-type mice (Fig. 2).

3.3. Deletion of LOX-1, myocardial injury and myocardial function

The basal values of cardiac hemodynamic parameters (HR, LVDP and $\pm dP/dt_{max}$) were similar in the wild-type and LOX-1 KO mice. In both groups of mice, sham I–R caused no significant changes in HR, LVDP and $\pm dP/dt_{max}$.

Following I–R, there was a marked decrease in all parameters of cardiac function in the wild-type mice. Reduction in both $+dP/dt_{max}$ and $-dP/dt_{max}$ reflects a decrease in global systolic and diastolic function, respectively. Importantly, despite similar period of I–R, there was much less deterioration of hemodynamic parameters indicating preservation of cardiac function in the LOX-1 mice ($P<0.01$ vs. wild-type mice) (Fig. 3).

In the wild-type mice, I–R resulted in extensive infarct (64.1 ± 10.6% of AAR). In contrast, LOX-1 KO mice had a much smaller infarct (23.4±3.5% of AAR, $P<0.01$). Similar reduction in injury was noted when infarct area was expressed as percent of LV (Fig. 4A).

Multiple myocardial sections were examined for histological evidence of injury. There were extensive areas of injury in the left coronary artery-supplied region in the wild-type mice. Much fewer and smaller areas of injury were observed in the LOX-1 KO mice hearts (Fig. 4B), consistent with the data shown in Fig. 4A. In the wild-type mice, many capillaries in the I–R regions were occluded with inflammatory cells, much less so in the LOX-1 KO mice (Fig. 4E). Reduced infiltration of inflammatory cells in the LOX-1 KO mice probably reflects the deletion of LOX-1 which as a leukocyte adhesion molecule.

In the wild-type mice, I–R resulted in a marked release of creatine kinase-MB (vs. sham I–R mice). Serum creatine kinase-MB levels were much lower in the LOX-1 KO mice ($P<0.01$, Fig. 4C), reflecting less myocyte death.

3.4. Myocardial ischemia–reperfusion and oxidative stress

Release of ROS during I–R causes peroxidation of lipids in the cell membrane [17]. As shown in Fig. 4D, I–R caused a significant increase in serum MDA levels in the wild-type mice. In contrast, LOX-1 KO mice had much lower MDA levels ($P<0.01$ vs. wild-type mice), indicating much less lipid peroxidation (Fig. 4D). I–R also increased the expression of nitrotyrosine, as an indirect marker of formation of peroxynitrite, in wild-type mice, but much less so in the LOX-1 KO mice (Fig. 5A). Interestingly, SOD activity was enhanced by I–R in the wild-type mice, and it increased further in the LOX-1 KO mice (Fig. 5B).

3.5. LOX-1 and redox-sensitive signaling

Recent studies show activation of MAPKs leads to an inflammatory and pro-oxidant state [18,19]. As shown in Fig. 6,

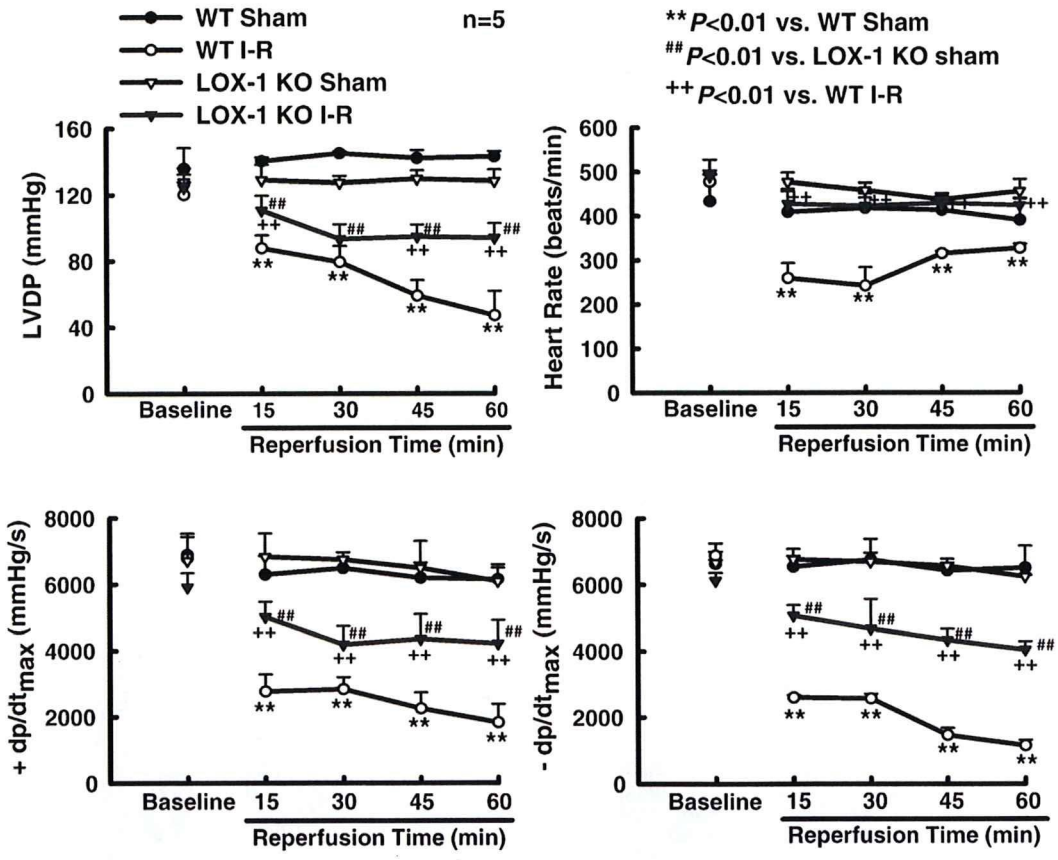

Fig. 3. Cardiac hemodynamics during ischemia–reperfusion. Heart rate (HR), left ventricular developed pressure (LVDP) and $\pm dP/dt_{max}$ were measured in the wild-type and LOX-1 KO mice subjected to ischemia–reperfusion (I–R). KO: knockout; WT: wild-type.

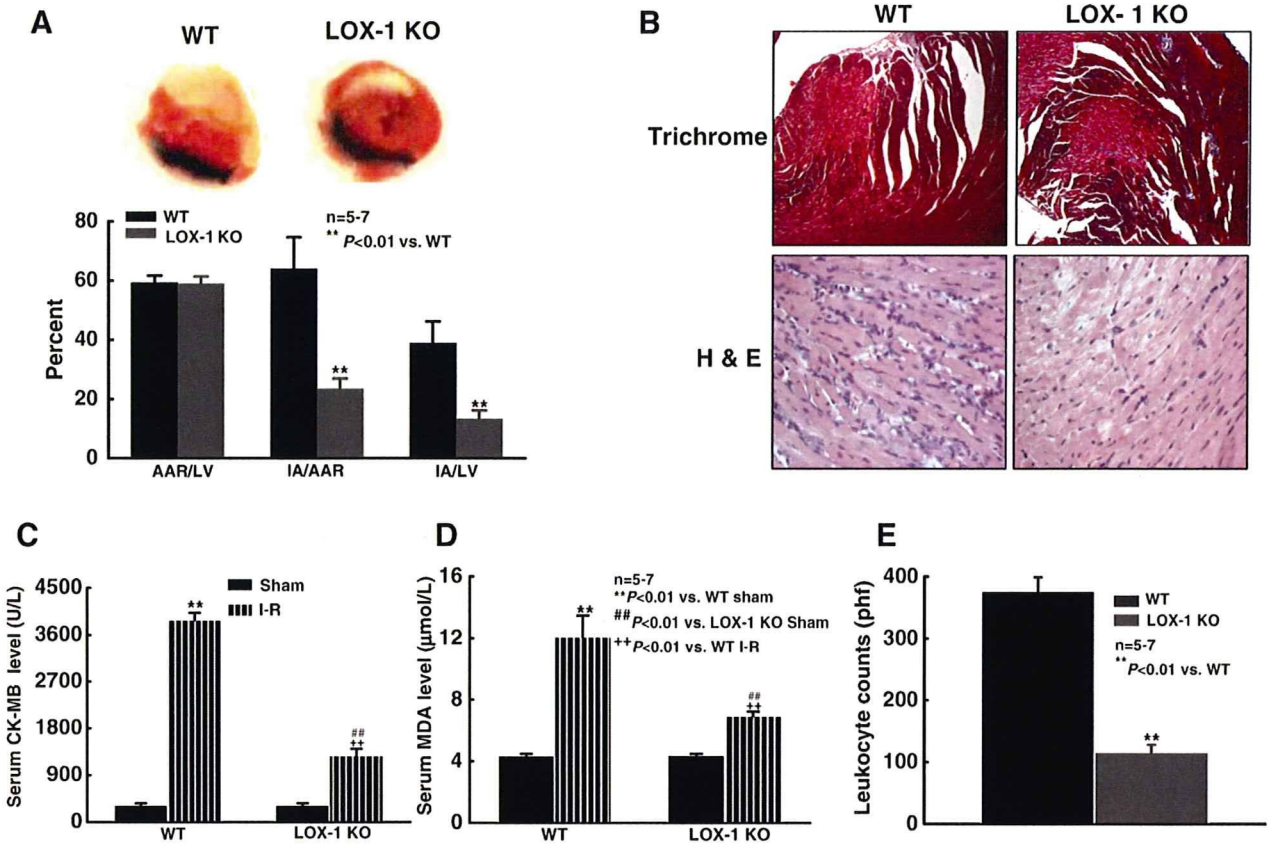

Fig. 4. Myocardial infarction, inflammation and serum levels of CK-MB and MDA. (A) Infarct size (IA) as percent of area at risk (AAR) and as percent of left ventricle (LV) in different groups of mice. (B) Representative myocardial sections stained with Masson's trichrome stain (upper panel) and H&E (lower panel) (original magnification, ×20). (C) Serum creative kinase-MB (CK-MB) level. (D) Serum malondialdehyde (MDA) level. (E) Quantitation of leukocyte infiltration in I–R regions. KO: knockout; I–R: ischemia–reperfusion; WT: wild-type.

protein levels of p38 and p44/42 MAPK were not altered during I–R; however, phosphorylation of p38MAPK (phos-p38MAPK) was enhanced by ~100% and that of p44/42 by ~60% in the wild-type mice subjected to I–R ($P<0.01$ vs. sham I–R mice). Phos-p38MAPK level was less in the basal state in the LOX-1 KO mice than in the wild-type mice and it increased only modestly during I–R ($P<0.01$ vs. wild-type mice). Importantly, phos-p44/42 MAPK increased in the LOX-1 KO mice during I–R, similar to that in the wild-type.

Akt-1 phosphorylates several proteins that promote cell injury and stimulates NOS activity [20,21]. Alterations in its activity are important in the phosphorylation of NOS and release

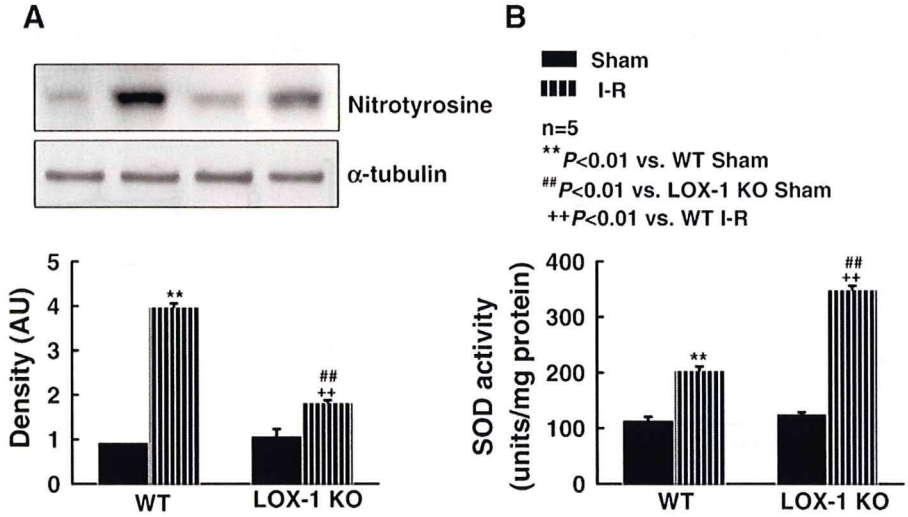

Fig. 5. Expression of nitrotyrosine and Cu/Zn superoxide dismutase (SOD) activity. KO: knockout; I–R: ischemia–reperfusion; WT: wild-type.

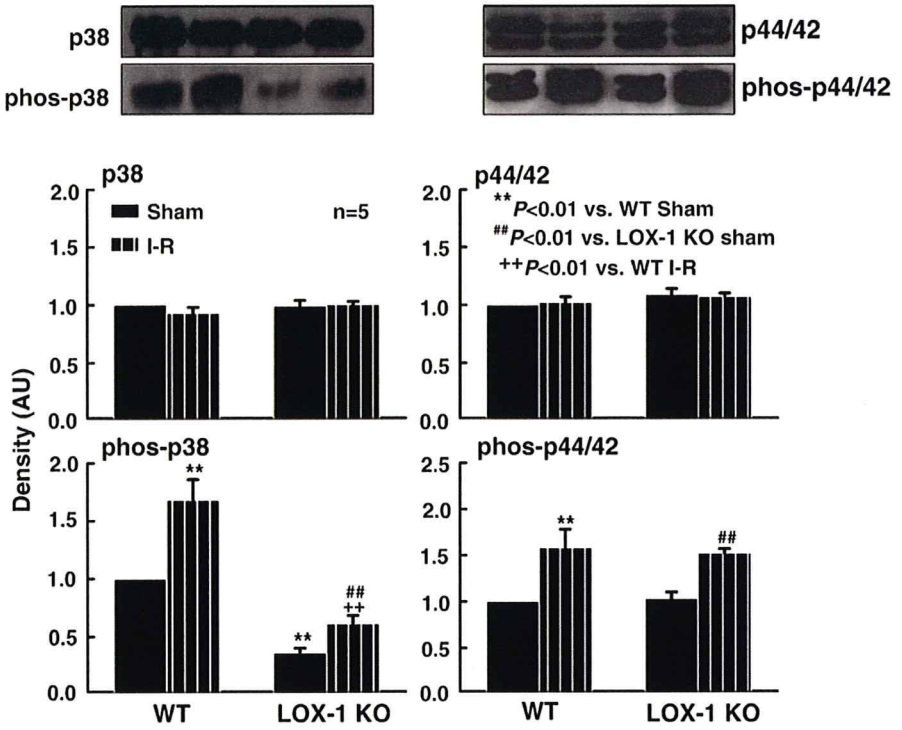

Fig. 6. Mitogen-activated protein kinases expression determined by Western analysis. KO: knockout; I–R: ischemia–reperfusion; WT: wild-type.

of NO in response to oxidant stimuli [20–22]. As shown in Fig. 7, Akt-1 levels were similar in the LOX-1 KO and wild-type mice at baseline. Phosphorylation of Akt-1 increased 84% during I–R in the wild-type mice ($P<0.01$ vs. sham control mice), but much less so (only 37%) in the LOX-1 KO mice ($P<0.01$ vs. wild-type mice). Interestingly, the basal levels of phosphorylated Akt-1 was lower in the LOX-1 KO mice ($P<0.01$ vs. wild-type mice).

Stimulation of iNOS results in release of large amounts of NO in the myocardium which can serve as an oxidant stimulus itself as well as in combination with superoxide anions resulting in the formation of peroxynitrite [23]. As shown in Fig. 8, the basal iNOS expression was lower in the LOX-1 KO mice ($P<0.01$ vs. wild-type mice). The expression of iNOS increased significantly during I–R in both wild-type and LOX-1 KO mice, but much less so in the LOX-1 KO mice ($P<0.01$). These data are consistent with the diminished levels of phosphorylated Akt-1 and nitrotyrosine in the LOX-1 KO mice (Fig. 6).

4. Discussion

Our study provides clear evidence for a critical role of LOX-1 in myocardial I–R injury, since I–R in the LOX-1 KO mice was associated with significantly less necrosis than in the wild-type mice. Reduction in necrosis with LOX-1 abrogation was accompanied with preservation of cardiac function, less lipid peroxidation and attenuated myocardial inflammatory response.

A major question that we addressed in this study was if LOX-1 is causally involved in the genesis of myocardial I–R injury. Reperfusion injury is associated with release of large amounts of ROS [2], which can oxidize lipids. Ox-LDL and ROS upregulate LOX-1 [10,12]. LOX-1 activation itself causes

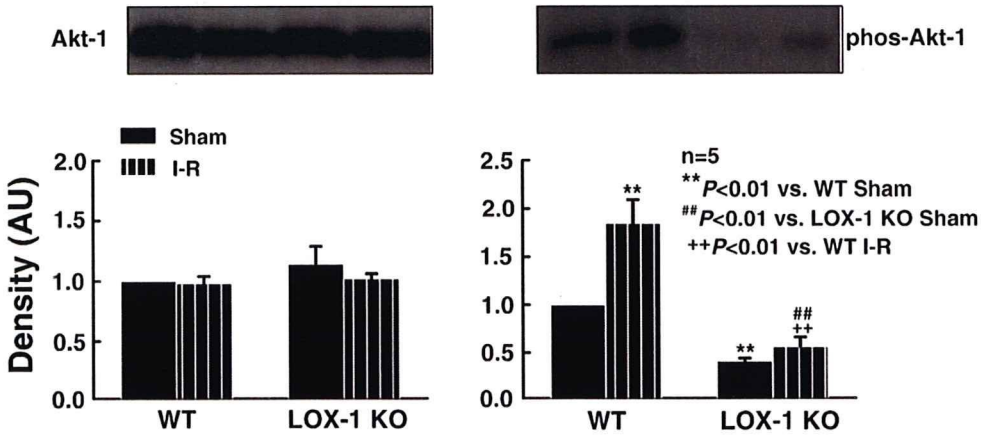

Fig. 7. Expression of Akt-1 determined by Western analysis. KO: knockout; I–R: ischemia–reperfusion; WT: wild-type.

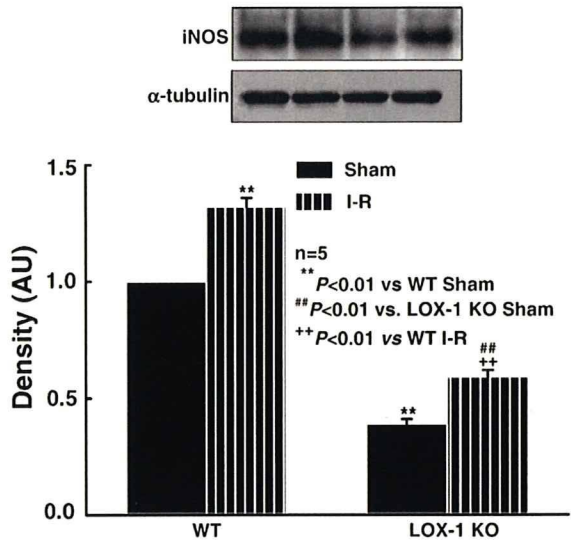

Fig. 8. Expression of iNOS determined by Western analysis. KO: knockout; I–R: ischemia–reperfusion; WT: wild-type.

release of ROS [11], implying a positive feedback between ROS, LOX-1 and oxidation of lipids. LOX-1 also acts as a leukocyte adhesion molecule, which promotes infiltration of inflammatory cells into tissues [24]. Other studies have shown that inhibition of ROS can limit reperfusion injury and associated inflammatory response [2]. Reperfusion injury is also associated with expression of the cytokine TNFα and activation of renin–angiotensin system resulting in the release of angiotensin II [25,26]. Both TNFα and angiotensin II have been shown to upregulate LOX-1 [27,28]. It is conceivable that the common link between various mediators of reperfusion injury is expression of LOX-1 that perpetuates the vicious cycle of lipid peroxidation, ROS release and inflammation.

Release of ROS during I–R results in the activation of MAPKs [19]. Recent data suggest that p38MAPK activation is critical in the genesis of inflammation in the I–R heart [18]. Kaiser et al [29] found that mice expressing a dominant-negative p38MAPK are significantly protected from I–R injury. Our observation of enhanced p38MAPK phosphorylation in association with cardiac inflammation, injury and functional impairment in the wild-type mice following I–R is in agreement with these studies. Attenuation of basal as well as I–R-stimulated phos-p38MAPK levels and preservation of cardiac function in the LOX-1 KO mice suggest that LOX-1 is an important mediator of ROS release, MAPK activation and cardiac injury and functional impairment. This concept is supported by previous studies in rats [13] in which I–R was associated with p38MAPK activation, and treatment of rats with LOX-1 antibody reduced p38MAPK activation. It is of note that the phos-p44/42 MAPK levels increased during I–R similarly in the wild-type and LOX-1 KO mice. Interestingly, Reid et al. [30] showed that cardioprotection mediated by adenosine receptor preconditioning was mediated by pre-ischemic phosphorylation of subcellular p44/42 MAPK, but that adenosine receptor preconditioning had no effect on p44/42 MAPK activation during reperfusion. In concert with these data [18,20,30], the present study shows that p38MAPK activation is an important pro-oxidant and pro-inflammatory signal during I–R in the wild-type mice and that this signal was blocked by LOX-1 abrogation.

We found iNOS and nitrotyrosine expression to be markedly increased following I–R in the wild-type mice. iNOS upregulation has been shown to be an important determinant of myocardial I–R injury in some studies [23], although studies in iNOS KO mice did not show myocardial preservation [31,32]. Release of large amounts of NO as a result of iNOS upregulation *per se* and via formation of peroxynitrite may exert direct cardio-suppressive effect [23,33]. Attenuation of iNOS and nitrotyrosine upregulation, and subsequent preservation of hemodynamic function in the LOX-1 KO mice during I–R suggest that iNOS activation may be linked to LOX-1 expression and myocardial dysfunction during ischemia.

We demonstrated intense activation of Akt-1 in the hearts of wild-type mice subjected to myocardial I–R, and much less in the LOX-1 KO mice. Several lines of evidence suggest a link between Akt-1 activation and iNOS expression/activation [20–22]. It has been shown that hypoxia-induced iNOS expression in microglia is regulated by PI3-kinase/Akt and p38MAPK activation [34,35]. Chen et al. [36] found that hypoxia–reoxygenation-induced myocyte injury was associated with increased Akt-1 phosphorylation and iNOS upregulation. Taken together, these data indicate that I–R induces iNOS in large part through the Akt pathway. Akt-1 has been shown to be a pro-survival mechanism [37]. Upregulation of Akt-1 after I–R may imply the body's attempt to generate "survival" signal. In keeping with the concept of survival signals during I–R, SOD activity increased in the wild-type mice, and it increased further in the LOX-1 KO mice. Studies in LRLR KO mice show that deletion of LOX-1 enhances SOD activity [16].

The basal levels of phos-Akt-1, iNOS, and phos-p38MAPK were lower in the LOX-1 KO mice as compared with the wild-type mice. Recently, we described enhanced endothelium-dependent relaxation and expression of endothelial NOS at baseline in LOX-1 KO mice [16], probably reflecting the enhanced NO levels. Increase in basal NO levels can inhibit iNOS transcription [38]. It is also well documented that Akt-1 and p38MAPK are redox-sensitive. Therefore, it is not surprising that the basal expression of iNOS, as well as the phosphorylation of Akt-1 and p38MAPK, is reduced in the LOX-1 KO mice. However, these postulates need to be further studied in these mice.

In summary, this study provides a link between ROS release, MAPK activation, and PI3-K/Akt/iNOS signaling in the overall determination of I–R injury. We believe that LOX-1 may be a potential therapeutic target in myocardial ischemic injury.

Acknowledgments

This study was supported in part by funds from the Department of Veterans Affairs (J.L.M.) the American Heart association (P.L.H.), and the Ministry of Education, Culture, Sports, Science and Technology of Japan; the Ministry of Health, Labor and Welfare of Japan; and the National Institute of Biomedical Innovation, Japan (T.S.).

References

[1] Buja LM. Myocardial ischemia and reperfusion injury. Cardiovasc Pathol 2005;14:170–5.

[2] Giordano FJ. Oxygen, oxidative stress, hypoxia, and heart failure. J Clin Invest 2005;115:500–8.

[3] Liao L, Harris NR, Granger DN. Oxidized low-density lipoproteins and microvascular responses to ischemia–reperfusion. Am J Physiol 1996;271: H2508–14.

[4] Stielow C, Catar RA, Muller G, Wingler K, Scheurer P, Schmidt HH, et al. Novel Nox inhibitor of oxLDL-induced reactive oxygen species formation in human endothelial cells. Biochem Biophys Res Commun 2006;344: 200–5.

[5] Liu YH, Carretero OA, Cingolani OH, Liao TD, Sun Y, Xu J, et al. Role of inducible nitric oxide synthase in cardiac function and remodeling in mice with heart failure due to myocardial infarction. Am J Physiol Heart Circ Physiol 2005;289:H2616–23.

[6] Harrison GJ, Jordan LR, Selley ML, Willis RJ. Low-density lipoproteins inhibit histamine and $NaNO_2$ relaxation of the coronary vasculature and reduce contractile function in isolated rat hears. Heart Vessels 1995;10:249–57.

[7] Ehara S, Ueda M, Naruko T, Haze K, Itoh A, Otsuka M, et al. Elevated levels of oxidized low density lipoprotein show a positive relationship with the severity of acute coronary syndromes. Circulation 2001;103:1955–60.

[8] Ekmekcioglu C, Mehrabi MR, Glogar HD, Jucewicz M, Volf I, Spieckermann PG. Oxidized low-density lipoprotein is localized in the ventricles of hearts from patients with coronary heart disease. Int J Clin Lab Res 2000;30:133–40.

[9] Moriwaki H, Kume N, Sawamura T, Takuma A, Hajime H, Hiroshi O, et al. Ligand specificity of LOX-1, a novel receptor for oxidized low-density lipoprotein. Arterioscler Thromb Vasc Biol 1998;18:1541–7.

[10] Nagase M, Ando K, Nagase T, Kaname S, Sawamura T, Fujita T. Redox-sensitive regulation of LOX-1 gene expression in vascular endothelium. Biochem Biophys Res Commun 2001;281:720–5.

[11] Cominacini L, Pasini AF, Garbin U, Davoli A, Tosetti ML, Campagnola M, et al. Oxidized low density lipoprotein (ox-LDL) binding to ox-LDL receptor-1 in endothelial cells induces the activation of NF-kappaB through an increased production of intracellular reactive oxygen species. J Biol Chem 2000;275:12633–8.

[12] Chen J, Mehta JL, Haider N, Zhang X, Narula J, Li D. Role of caspases in Ox-LDL-induced apoptotic cascade in human coronary artery endothelial cells. Circ Res 2004;94:370–6.

[13] Li D, Williams V, Liu L, Chen H, Sawamura T, Antakli T, et al. LOX-1 inhibition in myocardial ischemia–reperfusion injury: modulation of MMP-1 and inflammation. Am J Physiol Heart Circ Physiol 2002;283:H1795–801.

[14] Li D, Williams V, Liu L, Chen H, Sawamura T, Romeo F, et al. Expression of lectin-like oxidized low-density lipoprotein receptors during ischemia–reperfusion and its role in determination of apoptosis and left ventricular dysfunction. J Am Coll Cardiol 2003;41:1048–55.

[15] Hayashida K, Kume N, Murase T, Minami M, Nakagawa D, Inada T, et al. Serum soluble lectin-like oxidized low-density lipoprotein receptor-1 levels are elevated in acute coronary syndrome: a novel marker for early diagnosis. Circulation 2005;112:812–8.

[16] Mehta JL, Sanada R, Hu CP, Chen J, Dandapat A, Sugawara F, et al. Deletion of LOX-1 reduces atherogenesis in LDLR knockout mice fed high cholesterol diet. Circ Res 2007;100:1634–42.

[17] Rao PR, Kumar VK, Viswanath RK, Subbaraju GV. Cardioprotective activity of alcoholic extract of *Tinospora cordifolia* in ischemia–reperfusion induced myocardial infarction in rats. Biol Pharm Bull 2005;28:2319–22.

[18] Clerk A, Sugden PH. Inflame my heart (by p38-MAPK). Circ Res 2006;99:455–8.

[19] McCubrey JA, Lahair MM, Franklin RA. Reactive oxygen species-induced activation of the MAP kinase signaling pathways. Antioxid Redox Signal 2006;8:1775–89.

[20] Bae JH, Jang BC, Suh SI, Ha E, Baik HH, Kim SS, et al. Manganese induces inducible nitric oxide synthase (iNOS) expression via activation of both MAP kinase and PI3K/Akt pathways in BV2 microglial cells. Neurosci Lett 2006;398:151–4.

[21] Laskin DL, Fakhrzadeh L, Heck DE, Gerecke D, Laskin JD. Upregulation of phosphoinositide 3-kinase and protein kinase B in alveolar macrophages following ozone inhalation. Role of NF-kappaB and STAT-1 in ozone-induced nitric oxide production and toxicity. Mol Cell Biochem 2002;234–235:91–8.

[22] Kao SJ, Lei HC, Kuo CT, Chang MS, Chen BC, Chang YC, et al. Lipoteichoic acid induces nuclear factor-kappaB activation and nitric oxide synthase expression via phosphatidylinositol 3-kinase, Akt, and p38 MAPK in RAW 264.7 macrophages. Immunology 2005;115:366–74.

[23] Schulz R, Kelm M, Heusch G. Nitric oxide in myocardial ischemia/reperfusion injury. Cardiovasc Res 2004;61:402–13.

[24] Honjo M, Nakamura K, Yamashiro K, Kiryu J, Tanihara H, McEvoy LM, et al. Lectin-like oxidized LDL receptor-1 is a cell-adhesion molecule involved in endotoxin-induced inflammation. Proc Natl Acad Sci U S A 2003;100:1274–9.

[25] Belosjorow S, Bolle I, Duschin A, Heusch G, Schulz R. TNF-alpha antibodies are as effective as ischemic preconditioning in reducing infarct size in rabbits. Am J Physiol Heart Circ Physiol 2003;284:H927–30.

[26] Yang BC, Phillips MI, Ambuehl PE, Shen LP, Mehta P, Mehta JL. Increase in angiotensin II type 1 receptor expression immediately after ischemia–reperfusion in isolated rat hearts. Circulation 1997;96:922–6.

[27] Li DY, Sawamura T, Mehta JL. Upregulation of endothelial receptor for oxidized low-density lipoprotein (LOX-1) in cultured human coronary artery endothelial cells by angiotensin II type-1 receptor activation. Circ Res 1999;84:1043–9.

[28] Kume N, Murase T, Moriwaki H, Aoyama T, Sawamura T, Masaki T, et al. Inducible expression of lectin-like oxidized LDL receptor-1 in vascular endothelial cells. Circ Res 1998;83:322–7.

[29] Kaiser RA, Bueno OF, Lips DJ, Doevendans PA, Jones F, Kimball TF, et al. Targeted inhibition of p38 mitogen-activated protein kinase antagonizes cardiac injury and cell death following ischemia–reperfusion in vivo. J Biol Chem 2004;279:15524–30.

[30] Reid EA, Kristo G, Yoshimura Y, Ballard-Croft C, Keith BJ, Mentzer Jr RM, et al. In vivo adenosine receptor preconditioning reduces myocardial infarct size via subcellular ERK signaling. Am J Physiol Heart Circ Physiol 2005;288:H2253–9.

[31] Guo Y, Jones WK, Xuan YT, Tang XL, Bao W, Wu WJ, et al. The late phase of ischemic preconditioning is abrogated by targeted disruption of the inducible NO synthase gene. Proc Natl Acad Sci U S A 1999;96:11507–12.

[32] Xi L, Jarrett NC, Hess ML, Kukreja RC. Myocardial ischemia/reperfusion injury in the inducible nitric oxide synthase knockout mice. Life Sci 1999;65:935–45.

[33] Ferdinandy P, Schulz R. Nitric oxide, superoxide, and peroxynitrite in myocardial ischaemia–reperfusion injury and preconditioning. Br J Pharmacol 2003;138:532–43.

[34] Lu DY, Liou HC, Tang CH, Fu WM. Hypoxia-induced iNOS expression in microglia is regulated by the PI3-kinase/Akt/mTOR signaling pathway and activation of hypoxia inducible factor-1alpha. Biochem Pharmacol 2006;72:992–1000.

[35] Park SY, Lee H, Hur J, Kim SY, Kim H, Park JH, et al. Hypoxia induces nitric oxide production in mouse microglia via p38 mitogen-activated protein kinase pathway. Brain Res Mol Brain Res 2002;107:9–16.

[36] Chen H, Li D, Saldeen T, Mehta JL. TGF-beta1 modulates NOS expression and phosphorylation of Akt/PKB in rat myocytes exposed to hypoxia–reoxygenation. Am J Physiol Heart Circ Physiol 2001;281: H1035–9.

[37] Toth A, Kovacs K, Deres P, Halmosi R, Czopf L, Hanto K, et al. Impact of a novel cardioprotective agent on the ischaemia–reperfusion-induced Akt kinase activation. Biochem Pharmacol 2003;66:2263–72.

[38] Suzuki H, Colasanti M. Cross-talk between constitutive and inducible nitric oxide synthases. Circulation 2001;103:e81.